Journal of Experimental Botany, Vol. 64, No. 18, pp. 5569–5586, 2013
doi:10.1093/jxb/ert328 Advance Access publication 11 October, 2013
This paper is available online free of all access charges (see http://jxb.oxfordjournals.org/open_access.html for further details)

Journal of Experimental Botany
www.jxb.oxfordjournals.org

RESEARCH PAPER

Proteomic and phosphoproteomic analysis of polyethylene glycol-induced osmotic stress in root tips of common bean (*Phaseolus vulgaris* L.)

Zhong-Bao Yang[1,2], Dejene Eticha[3], Hendrik Führs[4], Dimitri Heintz[5], Daniel Ayoub[6], Alain Van Dorsselaer[6], Barbara Schlingmann[7], Idupulapati Madhusudana Rao[8], Hans-Peter Braun[9] and Walter Johannes Horst[2,*]

[1] The Key Laboratory of Plant Cell Engineering and Germplasm Innovation, Ministry of Education, College of Life Science, Shandong University, Jinan 250100, PR China
[2] Institute for Plant Nutrition, Leibniz Universität Hannover, Herrenhäuser Strasse 2, 30419 Hannover, Germany
[3] Yara GmbH, Hanninghof 35, 48249 Dülmen, Germany
[4] Applied Research and Advisory Service Agro, K+S KALI GmbH, Bertha-von-Suttner-Strasse 7, 34131 Kassel, Germany
[5] Institut de Biologie Moléculaire des Plantes (IBMP), 28 rue Goethe, CNRS-UPR2357, Université de Strasbourg, 67083 Strasbourg, France
[6] Laboratoire de Spectrométrie de Masse Bio-Organique, Université de Strasbourg, IPHC, 25 rue Becquerel, 67087 Strasbourg, France
[7] Institute of BioPhysics, Leibniz Universität Hannover, Herrenhäuser Strasse 2, D-30419 Hannover, Germany
[8] International Center for Tropical Agriculture (CIAT), AA 6713, Cali, Colombia
[9] Institute of Plant Genetics, Leibniz Universität Hannover, Herrenhäuser Strasse 2, D-30419 Hannover, Germany

* To whom correspondence should be addressed. E-mail: horst@pflern.uni-hannover.de

Received 14 May 2013; Revised 11 August 2013; Accepted 30 August 2013

Abstract

Previous studies have shown that polyethylene glycol (PEG)-induced osmotic stress (OS) reduces cell-wall (CW) porosity and limits aluminium (Al) uptake by root tips of common bean (*Phaseolus vulgaris* L.). A subsequent transcriptomic study suggested that genes related to CW processes are involved in adjustment to OS. In this study, a proteomic and phosphoproteomic approach was applied to identify OS-induced protein regulation to further improve our understanding of how OS affects Al accumulation. Analysis of total soluble proteins in root tips indicated that, in total, 22 proteins were differentially regulated by OS; these proteins were functionally categorized. Seventy-seven percent of the total expressed proteins were involved in metabolic pathways, particularly of carbohydrate and amino acid metabolism. An analysis of the apoplastic proteome revealed that OS reduced the level of five proteins and increased that of seven proteins. Investigation of the total soluble phosphoproteome suggested that dehydrin responded to OS with an enhanced phosphorylation state without a change in abundance. A cellular immunolocalization analysis indicated that dehydrin was localized mainly in the CW. This suggests that dehydrin may play a major protective role in the OS-induced physical breakdown of the CW structure and thus maintenance of the reversibility of CW extensibility during recovery from OS. The proteomic and phosphoproteomic analyses provided novel insights into the complex mechanisms of OS-induced reduction of Al accumulation in the root tips of common bean and highlight a key role for modification of CW structure.

Key words: Apoplast, cell wall, common bean, dehydrin, phosphoproteomics, proteomics, root tips.

Abbreviations: 2D-IEF, two-dimensional isoelectric focusing; ABA, abscisic acid; Al, aluminium; BSA, bovine serum albumin; CPC, cytosolic protein contamination; CW, cell wall; ESI, electrospray ionization; FITC, fluorescein isothiocyanate; LC, liquid chromatography; MS, mass spectrometry; NCBI, National Center for Biotechnology Information; OS, osmotic stress; PEG, polyethylene glycol.

Introduction

Common bean (*Phaseolus vlugaris* L.) is the major food legume for human nutrition worldwide and is a major source of calories and protein, particularly for people in low-income food-deficit countries in the tropics (Graham, 1978; Rao, 2001; Beebe, 2012). Under field conditions, common bean often experiences different abiotic stresses including drought, toxicities of aluminium (Al) and manganese, low soil fertility, and high temperatures (Thung and Rao, 1999; Ishitani *et al.*, 2004; Beebe, 2012). About 60% of common bean-growing areas in the world are affected by drought stress, consequently resulting in a low level of average global yield production (Graham and Ranalli, 1997; Beebe *et al.*, 2008).

In plants growing in dry soil, both shoot and root growth are hampered (Westgate and Boyer, 1985; Sharp *et al.*, 1988). An important feature of the root system response to soil drying is the maintenance of root elongation at low water potentials that can severely inhibit shoot growth (Sharp *et al.*, 2004; Yamaguchi and Sharp, 2010), thus facilitating water uptake from the subsoil (Sponchiado *et al.*, 1989; Serraj and Sinclair, 2002). Investigations of the spatial distribution of the response of root elongation to drought have indicated that elongation is preferentially maintained at the root apex (Sharp *et al.*, 2004; Yamaguchi and Sharp, 2010; Yamaguchi *et al.*, 2010). Physiological studies on the response of the primary root growth of maize to water stress have demonstrated the involvement of three possible mechanisms: osmotic adjustment, modification of cell-wall (CW) extension properties and abscisic acid (ABA) accumulation (Sharp *et al.*, 2004; Yamaguchi and Sharp, 2010). Water loss from the plant cells controls turgor pressure and directly affects the extensibility of the plant CW (Moore *et al.*, 2008). The effect of drought stress on CW structure and properties has been studied extensively in maize roots at physiological and molecular levels (Wu and Cosgrove, 2000; Fan and Neumann, 2004; Sharp *et al.*, 2004; Fan *et al.*, 2006; Poroyko *et al.*, 2007; Zhu *et al.*, 2007; Spollen *et al.*, 2008; Yamaguchi and Sharp, 2010).

Our previous physiological studies in common bean demonstrated that the polyethylene glycol (PEG)-induced osmotic stress (OS) reduction of CW porosity enhanced Al resistance by the reduction of Al accumulation in the root tips (Yang *et al.*, 2010), the main Al-sensitive root zone (Rangel *et al.*, 2007). A transcriptomic analysis indicated that, among the OS-regulated genes, CW synthesis and organization-related genes were mostly downregulated, of which the CW modification genes *XTH* (xyloglucan endotransglucosylase/hydrolase) and *BEG* (glucan endo-1,3-β-glucosidase or β-1,3-glucanase), and the structural protein hydroxyproline-rich glycoprotein (HRGP) were supposed to be involved in modification of CW porosity (Yang *et al.*, 2011, 2013). However, transcriptomic profiling sometimes fails to unequivocally reveal regulations of biological processes, for example due to gene redundancy or post-translational modifications (Toorchi *et al.*, 2009; Zörb *et al.*, 2010). Post-translational modifications, such as phosphorylation and glycosylation, can result in a dramatic increase in proteome complexity without a concomitant increase in gene expression (Jensen, 2004; Rose *et al.*, 2004; Jiang *et al.*, 2007). Therefore, in this study, a proteomic and phosphoproteomic approach was applied to: (i) better understand the PEG-induced changes of OS and CW-related proteins in the root tips of Al-sensitive common bean genotype VAX 1, and (ii) further classify the potential mechanisms of CW proteins involved in the adjustment of CW porosity.

Materials and methods

Plant materials and growing conditions

Seeds of common bean genotype VAX 1 (Al sensitive) were germinated on filter paper sandwiched between sponges. After 3 d, uniform seedlings were transferred to a continuously aerated simplified nutrient solution containing 5 mM $CaCl_2$, 1 mM KCl, and 8 µM H_3BO_3 (Rangel *et al.*, 2007). Plants were cultured in a growth chamber under controlled environmental conditions with a 16/8 h light/dark cycle, 27/25 °C day/night temperature, 70% relative air humidity, and a photon flux density of 230 µmol m^{-2} s^{-1} of photosynthetically active radiation at mid-plant height. The pH of the nutrient solution was gradually lowered to 4.5 within 2 d. The plants were then transferred into a simplified nutrient solution (see above) without or with PEG 6000 (Sigma-Aldrich Chemie, Steinheim, Germany). The osmotic potential of the PEG 6000 (150 g l^{-1}) solution was –0.60 MPa, measured with a cryoscopic osmometer (Osmomat 030; Gonotec, Berlin, Germany).

Measurement of root-elongation rate

Two hours before the treatment was initiated, tap roots were marked 3 cm behind the root tip using a fine point permanent marker (Sharpie blue; Stanford), which did not affect root growth during the experimental period. Afterwards, the plants were transferred into a simplified nutrient solution (see above) without or with PEG. Root elongation was measured after the treatment period using a millimetre scale.

Determination of cell sap osmotic potential

The root tip cell sap was extracted and measured according to Tabuchi *et al.* (2004) with modifications. After treating the plants with PEG (0 and 150 g l^{-1}) for 24 h, 30 root tips of 1 cm length were excised and transferred into microfiltration tubes with a membrane pore size of 0.45 µm (GHP Nanosep MF Centrifugal Device; Pall Life Sciences, Ann Arbor, USA) in a 1.5 ml plastic tube after removing the free solution on the surface of roots by brief centrifugation. The samples were immediately frozen in liquid nitrogen and stored at –80 °C until use. The root tips were thawed at room temperature, and then centrifuged at 5000*g* for 10 min at 4 °C. More than 50 µl of cell sap was obtained from 30 root tips. The osmotic concentration of the cell sap was determined with a cryoscopic osmometer (see above), and the osmotic potential was calculated according to the van't Hoff equation (Nobel, 1991): $\pi = -nRT$, where π is the osmotic potential, R the gas constant, T the absolute temperature, and n the molar concentration.

Extraction of total soluble protein

Approximately 200 root tips of 1 cm length were harvested after treating the plants without or with 150 g l^{-1} PEG for 24 h, and ground with a mortar and pestle in liquid nitrogen. The homogenized sample powder was suspended in 4 ml extraction buffer [500 mM Tris/HCl, 50 mM EDTA, 100 mM KCl, 700 mM sucrose, 25 mM sodium fluoride, 1 mM sodium molybdate, 50 mM sodium pyrophosphate, 2% (v/v) β-mercaptoethanol and protease inhibitor (1 tablet per

10 ml aliquot; Sigma-Aldrich Chemie)] and incubated for 10 min on ice. Afterwards, an equal volume of water-saturated phenol was added and incubated for another 10 min at room temperature on a rotary shaker. The aqueous and organic phases were separated by centrifugation for 10 min at 11 000*g* and 4 °C. The phenolic phase was re-extracted with an equal volume of extraction buffer and centrifuged again. Phenol phases were combined and supplemented with 5 vols of 0.1 M ammonium acetate in methanol and incubated overnight at –20 °C for protein precipitation. After centrifugation at 11 000*g* for 3 min at 4 °C, precipitated proteins were washed three times with ammonium acetate in methanol and finally with acetone. Pellets were air dried. Extracted proteins were redissolved in rehydration solution (see below) for two-dimensional gel electrophoresis analysis. The protein concentration of extracts were determined in rehydration solution using a 2-D Quant Kit© (GE Healthcare, Munich, Germany) according to the manufacturer's instructions.

Extraction of apoplastic proteins

Apoplastic proteins were extracted from control (no PEG) and PEG-treated root tips of 1 cm length of bean genotype VAX 1 for 24 h, according to the methods described by Zhu *et al.* (2006). Approximately 2000 root tips (1 cm length) were excised and transferred into 20 mM ice-cold K_2PO_4 solution (pH 6.0). The root tips were then rinsed twice with 0.01 M MES (pH 5.5) buffer and oriented vertically with the root apex at the top in a filter column with a membrane pore size of 0.45 µM (Macherey-Nagel, Düren, Germany). The filter column was placed into a vial and the whole assembly was held on ice. Twenty millilitres of ice-cold 0.01 M MES buffer (pH 5.5) containing 0.2 M KCl plus protease inhibitors (1 mM phenylmethylsulphonyl fluoride and 5 µl of protease inhibitor cocktail; Sigma) was added to the vial, submerging the plant tissue. The whole assembly containing the root tips was vacuum infiltrated at –50 kPa for 15 min and for another 5 min without vacuum. The vial was removed, drained, and excess buffer was blotted away from the root tips through the bottom of the filter column. The filter column with root tips was then transferred to a new vial and centrifuged for 15 min at 1000*g*. All steps were conducted on ice or in a cold room at 4 °C. Infiltration and centrifugation were then repeated twice. Apoplastic extracts of the resulting three fractions were combined in Vivaspin 6 Centrifugal Concentrators (5000 molecular weight cut-off PES; Vivascience, UK) and centrifuged for 2 h at 5000*g*. Precipitation of apoplastic proteins was done as described in the previous section.

In each fraction of apoplastic protein extract, the activity of malate dehydrogenase (MDH), a commonly accepted marker for cytosolic contamination, was assayed according to Bergmeyer and Bernt (1974) and the protein yield was quantified according to Bradford (1976).

Two-dimensional isoelectric focusing (2D-IEF)/SDS-PAGE

2D-IEF/SDS-PAGE was carried out as described by Führs *et al.* (2008). For IEF, the IPGphor system (GE Healthcare) and immobiline DryStrip gels (18 cm) with a non-linear pH gradient of 3–11 (for total soluble and apoplastic proteins) or 4–7 (for total soluble phosphoproteins) were used. Proteins (about 1000 and 80 µg for total and apoplastic soluble proteins, respectively) were dissolved in rehydration solution [8 M urea, 2% (w/v) CHAPS, 0.5% (v/v) carrier ampholyte mixture (IPG buffer pH 3–11 or 4–7 NL; GE Healthcare), 50 mM dithiothreitol, 12 µl ml^{-1} of DeStreak (GE Healthcare) and a trace of bromophenol blue] and loaded onto individual gel strips. Focusing was done according to Werhahn and Braun (2002). Afterwards, the focused IPG strips were incubated with equilibration solution [50 mM Tris/HCl (pH 8.8), 6 M urea, 30% (v/v) glycerol, 2% (w/v) SDS, and bromophenol blue] supplemented with either 1% (w/v) dithiothreitol or 2.5% (w/v) iodoacetamide each for 15 min. The strips were then placed horizontally onto second-dimension SDS gels and the proteins separated according to Schägger and von Jagow (1987). Afterwards, for total soluble and apoplastic proteins, 2D gels were stained with colloidal Coomassie blue (CBB) G250 according to Neuhoff *et al.* (1985, 1990).

For phosphoprotein detection, 2D gels were stained using the Pro-Q Diamond Phosphoprotein Stain (Pro-Q DPS; Molecular Probes) according to Agrawal and Thelen (2009). Each treatment consisted of three independent biological replicates.

Image acquisition, image analysis, and statistical analysis

Image acquisition of CBB-stained gels was done using an Epson Expression 1600 scanner (Epson, Mehrbusch, Germany) at 300 dpi. Images were stored as TIFF files. Phosphoprotein detection on gels was done using a Typhoon™ Variable Mode Imager using 532 nm excitation and 580 nm bandpass emission filters at 100 µm resolution. Images were stored as 16-bit TIFF files (Agrawal and Thelen, 2009). 2D gel image analysis of CBB- and phosphoprotein-stained gels was carried out using ImageMaster™ 2D Platinum Software 6.0 (GE Healthcare). To compensate for variability owing to sample loading, gel staining and destaining, relative spot volumes were calculated (ratio of individual spot volume and total volume of all spots). In this study, significantly changed proteins between treated and control plants were defined as proteins that were more or less abundant by a factor of 1.5 or 0.67, respectively, with $P \leq 0.05$ (Student's *t*-test) unless otherwise specified.

Mass spectrometry (MS) analysis and data interpretation

After manually picking of protein spots with changed abundance, each spot was dried under vacuum. In-gel digestion was performed with an automated protein digestion system (MassPREP Station; Micromass, Manchester, UK). The gel slices were washed three times in a mixture containing 25 mM NH_4HCO_3:CH_3CN (1:1, v/v). The cysteine residues were reduced by the addition of 50 µl of 10 mM dithiothreitol at 57 °C and alkylated by the addition of 50 µl of 55 mM iodacetamide. After dehydration with acetonitrile, the proteins were cleaved in the gel with 40 µl of 12.5 ng $µl^{-1}$ modified porcine trypsin (Promega, Madison, WI, USA) in 25 mM NH_4HCO_3 at room temperature for 14 h. The resulting tryptic peptides were extracted with 60% acetonitrile in 0.5% formic acid, followed by a second extraction with 100% (v/v) acetonitrile.

Nano-liquid chromatography (LC)-MS/MS analysis of the resulting peptides was performed using an Agilent 1100 series HPLC-Chip/MS system (Agilent Technologies, Palo Alto, USA) coupled to an HCT Ultra ion trap (Bruker Daltonics, Bremen, Germany). Chromatographic separations were conducted on a chip containing a Zorbax 300SB-C18 column (75 µm inner diameter×150 mm) and a Zorbax 300SB-C18 (40 nl) enrichment column (Agilent Technologies).

The HCT Ultra ion trap was calibrated externally with standard compounds. The general MS parameters were as follows: capillary voltage, –1750 V; dry gas, 3.0 l min^{-1}; and dry temperature, 300 °C. The system was operated with automatic switching between MS and MS/MS modes. The MS scanning was performed in the standard-enhanced resolution mode at a scan rate of 8100 m/z s^{-1} with an aimed ion charge control of 100 000 in a maximal fill time of 200 ms, and a total of four scans were averaged to obtain an MS spectrum. The three most abundant peptides and preferentially doubly charged ions were selected on each MS spectrum for further isolation and fragmentation. The MS/MS scanning was performed in the ultrascan resolution mode at a scan rate of 26 000 m/z s^{-1} with an aimed ion charge control of 300 000, and a total of six scans were averaged to obtain an MS/MS spectrum. The complete system was fully controlled by ChemStation Rev. B.01.03 (Agilent Technologies) and EsquireControl 6.1 Build 78 (Bruker Daltonics) software. Mass data collected during LC-MS/MS analyses were processed using the software tool DataAnalysis 3.4 Build 169 and converted into.mgf files. The MS/MS data were analysed using MASCOT 2.2.0. (Matrix Science, London, UK) to search against an in-house-generated

protein database composed of protein sequences of Viridiplantae downloaded from http://www.ncbi.nlm.nih.gov/sites/entrez (on 6 March 2008) concatenated with reversed copies (decoy) of all sequences (23 478 588 entries). Spectra were searched with a mass tolerance of 0.5 Da for MS and MS/MS data, allowing a maximum of one missed cleavage by trypsin and with carbamidomethylation of cysteines, oxidation of methionines, and N-terminal acetylation of proteins specified as variable modifications. Protein identifications were validated when at least two peptides with high-quality MS/MS spectra (Mascot ion score >31) were detected. In the case of one-peptide hits, the score of the unique peptide must be greater (minimal 'difference score' of 6) than the 95% significance Mascot threshold (Mascot ion score >51). For the estimation of the false-positive rate in protein identification, a target-decoy database search was performed (Elias and Gygi, 2007).

Protein identifications by MS only were carried out for one of the three gel replicates, because gels obviously were very similar. Also, all analyses allowed us to identify unambiguously proteins of the expected molecular mass range.

Cellular immunolocalization of dehydrin

After treating the 3-d-old seedlings of common bean genotype VAX 1 without or with PEG 6000 (150 g l^{-1}) in the simplified nutrient solution (pH 4.5) for 24 h, transverse sections (~100–300 µm) of root segment (1–3, 3–6, and 6–9 mm from the root apex) were free-hand sectioned with a razor blade and collected in a fixative solution containing 4% paraformaldehyde in 50 mM PIPES, 5 mM $MgSO_4$, and 5 mM EGTA (pH 6.9). For the plasmolysis of cells, the free-hand-sectioned transverse root sections were first incubated in 0.8 M manitol for 30 min on ice before transferring them to the fixative solution. After 1–2 h of fixation at room temperature, the samples were washed repeatedly with PBS (pH 7.4) and blocked with 0.2% bovine serum albumin (BSA) in PBS for 30 min. The samples were then incubated in a diluted (1:100) solution of primary antibody (rabbit polyclonal anti-dehydrin; Agrisera, Sweden) overnight at 4 °C. The antibody dilution was made with PBS containing 0.2% BSA. The primary antibody was thoroughly washed off the samples with PBS three times for 5 min each. Next, they were incubated for 2 h in the presence of a 50-fold-diluted solution of the secondary antibody, anti-rabbit IgG coupled with fluorescein isothiocyanate (FITC) (Acris Antibodies, Germany). The samples were washed as described above, mounted on glass slides, and examined under a confocal laser-scanning microscope (Leica TCS SP2; Leica Microsystems, Heidelberg, Germany). Images were captured using Leica Confocal Software.

One dimensional (1D) SDS-PAGE and fluorescent western blotting

Approximately 50 root tips of 1 cm length were harvested after treating the plants without or with 150 g l^{-1} PEG for 24 h, and ground with a mortar and pestle in liquid nitrogen. The proteins were fractionated in three steps: (i) the homogenized sample powder was suspended in 200 µl of extraction buffer (see above) and incubated for 10 min on ice, then centrifuged at 12 000*g* for 15 min and the supernatant collected as fraction I; (ii) the remaining residue was resuspended in 200 µl of extraction buffer (see above) and incubated for 10 min on ice, then centrifuged at 12 000*g* for 15 min to wash the water-soluble proteins away, and the supernatant collected as fraction II; (iii) the remaining residue after step (i)i was resuspended in 200 µl of extraction buffer (see above) containing 1% SDS (to solubilize the hydroponic membrane protein), and incubated for 10 min and then centrifuged at 12 000*g* for 15 min, and the supernatant collected as fraction III. The proteins were precipitated with ammonium acetate and redissolved in rehydration solution. The protein concentration of extracts was determined using a 2-D Quant Kit© (GE Healthcare) according to the manufacturer's instructions. Approximately 45, 7, and 4 µg of proteins in fractions I, II, and III was obtained, respectively.

The same volume of the extracted proteins in fractions II and III with fraction I in each corresponding sample (~20, 3, and 2 µg proteins in fractions I, II, and III, respectively) was loaded onto the gel and electrophoretically separated in 12% separating and 4% stacking polyacrylamide gel, and then transferred to a nitrocellulose membrane. After blocking in TBS/Tween 20 containing 1% BSA, the blot was treated with the primary antibody (rabbit polyclonal anti-dehydrin) diluted 1:1000, followed by the secondary antibody (anti-rabbit IgG–FITC) diluted 1:500 separately. Photographs were obtained with a Bio-Imaging System MF-ChemiBIS 4.2 (Benthold, Bad Wildbad, Germany).

To determine the effect of PEG on the abundance of dehydrin protein, CBB-stained Rubisco was used as a loading control in addition to protein quantification. There was no difference between the PEG treatments (data not shown), suggesting that PEG did not affect the abundance of dehydrin.

Statistical analysis

A completely randomized design was used, with 4–12 replicates in each experiment. If not mentioned otherwise, statistical analysis was carried out using SAS 9.2. Means were compared using a *t*-test or Tukey test depending on the number of treatments being compared. *, **, ***, and ns denote significant differences at $P<0.05$, $P<0.01$, $P<0.001$, and not significant, respectively.

Results

Root-elongation rate of bean genotype VAX 1 was inhibited by 31% by a 24 h exposure to 150 g l^{-1} PEG (pH 4.5) in the simplified nutrient solution (Fig. 1A). Since cell expansion is determined by osmotic potential as well as CW extensibility in the root cells, and osmotic adjustment plays a major role in plant adaptation to OS, the osmotic potential of the root cells was measured using an osmometer. The osmotic potential of the cell sap of the root tips was decreased by 24 h treatment with 150 g l^{-1} of PEG from –0.55 to –0.96 MPa (Fig. 1B), suggesting osmotic adjustment of root cells by accumulating osmolytes facilitating water uptake into cells and thus adaptation to PEG-induced OS.

To identify the proteins affected by short-term (24 h) PEG-induced OS, the total soluble proteins were extracted from control (–PEG) and PEG-treated root tips. A total of 716 spots were detected after 2D-IEF/SDS-PAGE and CBB staining. Using specific threshold parameters (see Materials and methods), 22 proteins were identified exhibiting differential abundance due to the PEG treatment (Fig. 2A). Nine of these proteins showed higher and 13 proteins showed lower abundance in PEG-treated roots than in control (–PEG) roots (Fig. 2B, C). Close-ups of gel regions containing proteins of differential abundance are shown in Supplementary Fig. S1 (at *JXB* online).

The 22 differentially expressed proteins were analysed by *de novo* peptide sequencing using electrospray ionization (ESI)-MS/MS and identified by sequence comparisons using the National Center for Biotechnology Information (NCBI) protein database (Table 1). The identified 22 proteins were classified according to their proposed biological functions using the UniProt database (Table 1, Supplementary Fig. S2 at *JXB* online). Among the nine increased proteins, the functional

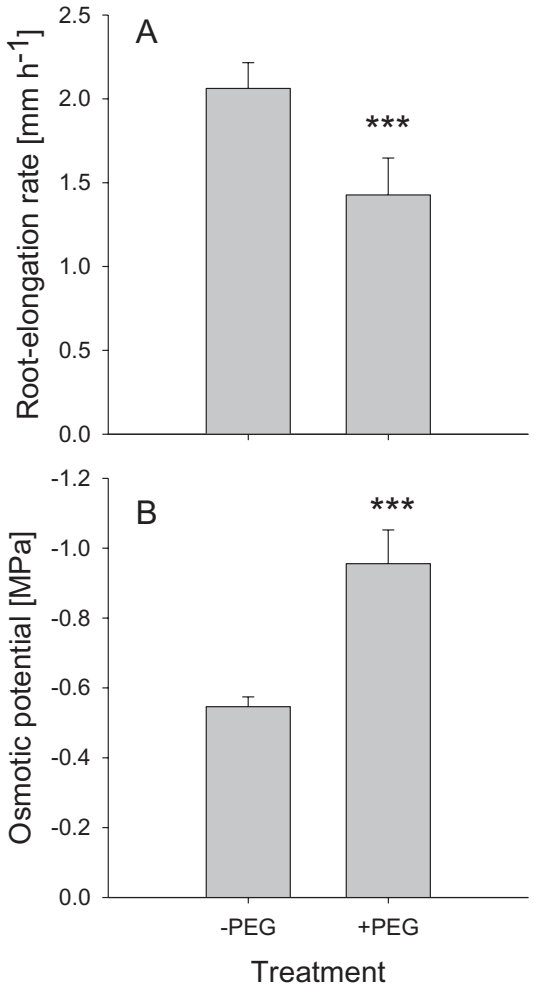

Fig. 1. Root-elongation rate (A) and cell sap osmotic potential (B) of 1 cm root tips of the common bean genotype VAX 1 under OS (left column, 0; right column –0.60 MPa osmotic potential). Plants were pre-cultured in a simplified nutrient solution containing 5 mM $CaCl_2$, 1 mM KCl, and 8 µM H_3BO_3 for 48 h for acclimation and pH adaptation, and then treated without or with PEG (150 g l^{-1}) in the simplified nutrient solution (pH 4.5) for 24 h. Bars represent means ±SD, n=12, for (A) and n=4 for (B). *** denotes significant differences between the +PEG treatment and the –PEG control at $P < 0.001$.

categories of carbohydrate metabolism, amino acid metabolism, protein processing, transcription, and unknown were represented by 45, 22, 11, 11, and 11%, respectively. Among the 13 decreased proteins (shown in Table 1), the functional categories of carbohydrate metabolism, amino acid metabolism, other metabolisms, stress response/defence, and protein processing were represented by 38, 31, 15, 8, and 8%, respectively. The functional classification of the identified increased and decreased proteins showed that the majority of the proteins (77%) were involved in pathways of primary metabolism (acetoacetyl-CoA thiolase, fructokinase, *myo*-inositol 1-phosphate synthase, phosphoglycerate mutase, fructokinase-like protein, alcohol dehydrogenase Adh-1, enolase, and NADPH-specific isocitrate dehydrogenase in carbohydrate metabolism; *S*-adenosylmethionine synthetase, D-3-phosphoglycerate dehydrogenase, and methionine synthase in amino acid metabolism), suggesting a pivotal importance of the primary metabolism in the response and adaptation of root tips to PEG-induced OS.

To investigate the effect of OS on the regulation of CW proteins of root tips of common bean, soluble and ionically bound apoplastic proteins were extracted and analysed. First, we tested the capability and efficiency of KCl as an extractant of CW proteins from root tips of common bean. Different concentrations were tested for their effect on CW protein yield and cytosolic protein contamination (CPC). The CPC was assessed by measuring MDH activity. CW proteins extracted with 0.1 M KCl did not show CPC in each of three sequential extractions; however, the protein yield was low. Infiltration with 0.4 M KCl yielded a great amount of protein but also resulted in a high CPC in the first infiltration step (data not shown). Therefore, to obtain a high protein yield with minimum CPC, 0.2 M KCl was chosen for extracting CW proteins from PEG-treated root tips of common bean (Table 2). This KCl concentration of 0.2 M has been used previously to extract CW proteins from the root-elongation zone of maize (Zhu *et al.*, 2006). Compared with the non-extractable proteins (tightly bound apoplastic proteins and symplastic proteins), MDH activity in the free and CW loosely bound protein fraction was low (Table 2), indicating only low-level contamination. PEG treatment (150 g l^{-1}) reduced the amount of extractable apoplastic protein in the root tips (Table 2).

2D-IEF/SDS-PAGE and subsequent staining with CBB showed that individual proteins could be visualized in spite of the low amount of CW proteins (80 µg) loaded on each gel (Fig. 3). On average, a total of 171 spots were detected on gels containing proteins extracted from PEG-treated and control (–PEG) root tips. A total of 13 proteins were significantly affected by PEG-induced OS. Of these, five and eight proteins showed lower and higher abundance in PEG-treated root tips, respectively (Fig. 3). ESI-MS/MS analysis of these 13 spots allowed the identification of eight proteins by BLAST search at the NCBI protein database (Table 3). Two of the proteins (fructokinase and pathogenesis-related protein 1) were reduced and six proteins (β-xylosidase, pectinacetylesterase precursor, serine hydroxymethyltransferase, serine carboxypeptidase, and fructose-1,6-bisphosphate aldolase) increased in abundance by PEG-induced OS (Table 3). Close-ups of the gels are shown in Supplementary Fig. S3 at *JXB* online.

The PEG-induced changes of phosphorylated and dephosphorylated proteins in root tips were examined by a phosphoproteomic approach using 2D-IEF/SDS-PAGE and Pro-Q DPS staining. Out of the identified 10 significantly changed proteins, seven showed increased phosphorylation (glucose-6-phosphate isomerase, actin, dehydrin, and lactoylglutathione lyase) and three proteins decreased phosphorylation (Ser/Thr-specific protein phosphatase 2A, regulatory subunit β isoform, pyruvate kinase, and branched-chain amino acid aminotransferase) in response to PEG-induced OS (Fig. 4A, Table 4). Close-ups of three of these proteins with high abundance are shown in Fig. 4B and were identified as belonging to the same protein family, dehydrin. The close-ups of all differentially formed proteins in response to PEG treatment are presented in Supplementary Fig. S4 at *JXB* online.

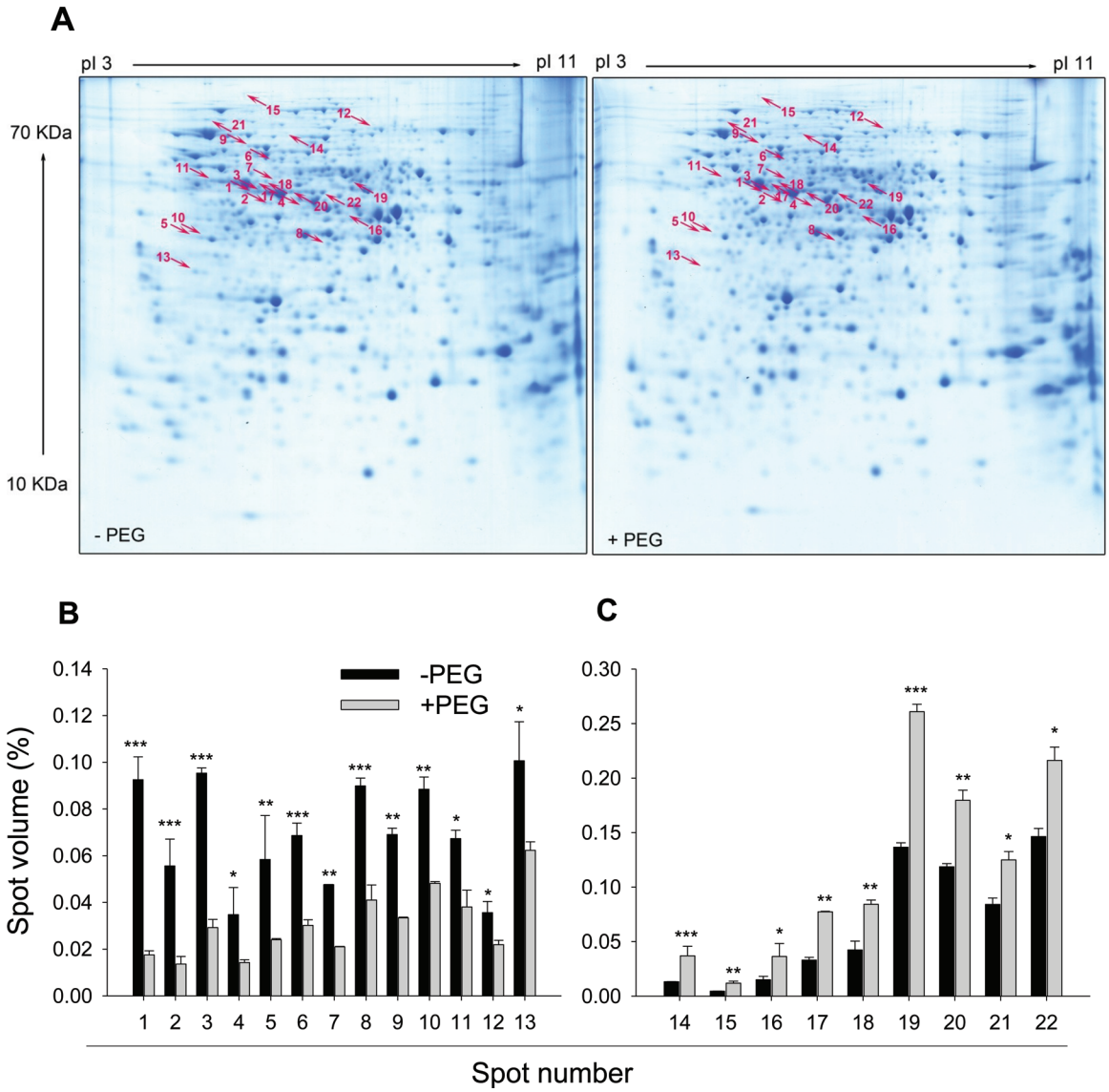

Fig. 2. Representative CBB-stained 2D-IEF/SDS-PAGE gels of total soluble proteins (A) and the relative spot volumes of the 22 significantly decreased (B) and increased (C) protein spots in control (–PEG) and PEG-treated root tips of common bean genotype VAX 1. Plants were pre-cultured in a simplified nutrient solution containing 5 mM $CaCl_2$, 1 mM KCl, and 8 μM H_3BO_3 for 48 h for acclimation and pH adaptation, and then treated without or with PEG (150 g l^{-1}) in the simplified nutrient solution (pH 4.5) for 24 h. Proteins were extracted from the root tips, separated by 2D-IEF/SDS-PAGE, and stained by CBB. Treatment-affected spots were marked by arrows and numbered consecutively. Three independent biological replications of each treatment were analysed using Image Master™ 2D PLATINUM Software 6.0. In (B) and (C), bars represent means ±SD, n=3. *, **, and *** denote significant PEG treatment differences at P<0.05, P<0.01, and P<0.001, respectively. (This figure is available in colour at *JXB* online.)

Gene analysis by quantitative real time-PCR (Livak and Schmittgen, 2001) indicated that PEG did not affect the transcriptional regulation of the gene *DHN* (GeneBank accession no. U54703), encoding the dehydrin protein, in the root tips of common bean (data not shown).

In a next step, the dehydrin protein was localized in the root apical 0–3, 3–6, and 6–10 mm segments using immunofluorescence (Fig. 5). In the absence of PEG, dehydrin primarily localized in the central cylinder, while the signal intensity in the epidermis and cortex was relatively weak, particularly in the 3–6 mm region (Fig. 5A–C, G–I). However, when roots were subjected to PEG stress, the signal intensity, particularly in the 3–6 mm region, was highly enhanced in the epidermis and cortex of all three root apical regions (Fig. 5D–F, J–L). High resolution of the cross-sections in PEG-treated 3–6 mm root apical region shows that dehydrin was localized in the CW or plasma membrane (Fig. 5M, N). To confirm whether dehydrin localized in the CW or plasma membrane, a high concentration of manitol (0.8 M) was used to induce plasmolysis of cells. The unchanged localization of dehydrin before and after plasmolysis (Fig. 5O, P) suggested that dehydrin is most probably localized in the CW.

To verify the primary localization of dehydrin in the CW, we fractionally extracted the root apical protein with and

Table 1. *List of the 22 proteins with significantly different abundance in the root tips of common bean genotype VAX 1 in response to PEG*

Plants were pre-cultured in a simplified nutrient solution containing 5 mM $CaCl_2$, 1 mM KCl, and 8 μM H_3BO_3 for 48 h for acclimation and pH adaptation, and then treated without or with PEG (150 g l^{-1}) in the simplified nutrient solution (pH 4.5). These 22 protein spots are shown in the CBB-stained 2D-IEF/SDS-PAGE gels in Fig. 2 and Supplementary Fig. S1. Spot no. relates to the corresponding spot number of Figs 2 and S1. FC, fold change (the relative protein spot volume of +PEG treatment to the relative protein spot volume of –PEG treatment). The proteins were identified by nano LC-MS/MS and BLASTed in the NCBI database. The protein functions were categorized based on the UniProt database and KEGG pathway. NI, not identified; MW, molecular weight. See Supplementary Table S1 at JXB online for further details.

Spot No.	Identity	MW (Da)	GenBank acc. no.	FC
Carbohydrate metabolism				
4	Acetoacetyl-CoA thiolase (*Medicago sativa*)	41 659.8	ACX47470	0.410
5	Fructokinase (*Arachis hypogaea*)	20 047.7	ACF74294	0.411
7	*myo*-Inositol 1-phosphate synthase (*Phaseolus vulgaris*)	56 431.4	CAH68559	0.441
9	Phosphoglycerate mutase (*Solanum tuberosum*)	60 271.9	AAD24857	0.484
10	Fructokinase-like protein (*Cicer arietinum*)	26 092.1	CAD31714	0.544
16	Alcohol dehydrogenase Adh-1 (*Glycine max*)	34 407.4	AAC62469	2.425
17	Enolase (*Glycine max*)	47 701.9	AAS18240	2.341
18	Enolase (*Glycine max*)	47 701.9	AAS18240	1.986
22	NADPH-specific isocitrate dehydrogenase (*Glycine max*)	49 124.2	AAA33978	1.500
Amino acid metabolism				
1	*S*-Adenosylmethionine synthetase (*Phaseolus lunatus*)	43 041.9	BAB83761	0.190
2	Methionine adenosyltransferase (*Pisum sativum*)	40 958.3	CAA57581	0.245
3	*S*-Adenosylmethionine synthetase (*Phaseolus lunatus*)	43 041.9	BAB83761	0.307
6	D-3-phosphoglycerate dehydrogenase. putative (*Ricinus communis*)	63 086.7	EEF43612	0.440
20	*S*-Adenosylmethionine synthetase (*Phaseolus lunatus*)	43 041.9	BAB83761	1.514
21	Methionine synthase (*Glycine max*)	84 266.4	AAQ08403	1.500
Other metabolisms				
12	1-Deoxyxylulose 5-phosphate synthase (*Chrysanthemum x morifolium*)	71 701.7	BAE79547	0.615
13	Inorganic pyrophosphatase, putative (*Ricinus communis*)	33 895.5	EEF44062	0.619
Stress response/defence				
8	Chloroplast thylakoid-bound ascorbate peroxidase (*Vigna unguiculata*)	39 791.4	AAS55852	0.596
Protein processing				
11	Tubulin A (*Glycine max*)	49 552.7	AAX86047	0.566
19	26S proteasome regulatory particle triple-A ATPase subunit1 (*Oryza sativa* Japonica group)	46 667.0	BAB17624	1.910
Transcription				
14	Pre-mRNA-splicing factor SLU7-A *(Arabidopsis lyrata* subsp. Lyrata)	61 961.8	EFH64697	2.794
Unknown				
15	NI	–	–	2.625

Table 2. *Yield of 0.2 mM KCl-extractable apoplastic proteins and the MDH activity (indicator of cytosolic contamination) of extracts from 1 cm root tips of common bean genotype VAX 1 grown in absence and presence of PEG 6000 for 24 h*

Root tips were three times consecutively infiltrated. The residue included tightly bound, non-extractable apoplastic and symplastic proteins.

PEG treatment (g l^{-1})	Infiltration step	Protein yield (ng per 1 cm root tip)	MDH activity (nmol min^{-1} per 1 cm root tip)
0	I	33.68 ± 5.45	0.10 ± 0.02
	II	29.06 ± 7.66	0.05 ± 0.02
	III	28.86 ± 7.34	0.06 ± 0.03
	Residue	251.19 ± 119.23	0.94 ± 0.54
150	I	21.39 ± 3.01	0.05 ± 0.01
	II	21.51 ± 9.46	0.06 ± 0.03
	III	19.60 ± 7.16	0.04 ± 0.02
	Residue	379.68 ± 212.15	0.58 ± 0.10

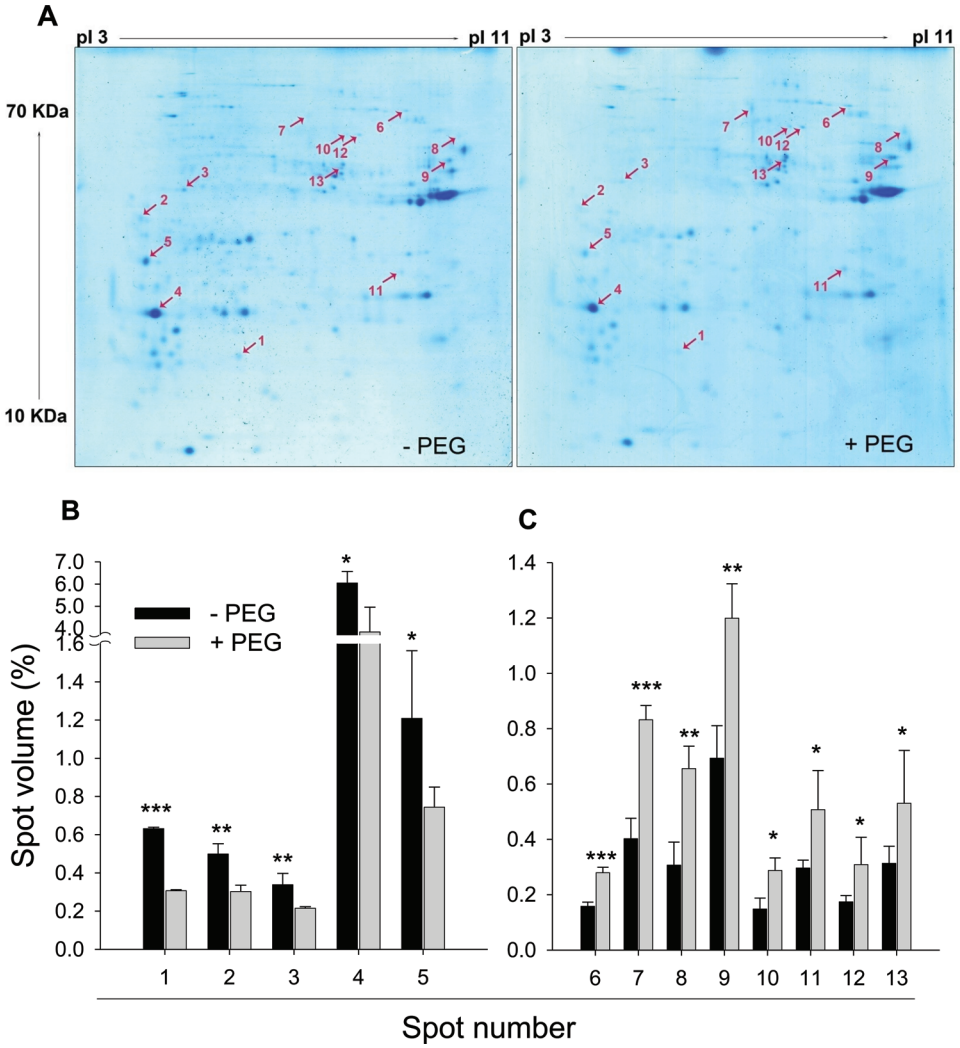

Fig. 3. Representative CBB-stained 2D-IEF/SDS-PAGE gel images of apoplastic proteins (A) and the relative volume of the 13 significantly decreased (B) and increased (C) apoplastic protein spots in control (–PEG) and PEG-treated root tips of common bean genotype VAX 1. Plants were pre-cultured in a simplified nutrient solution containing 5 mM $CaCl_2$, 1 mM KCl, and 8 μM H_3BO_3 for 48 h for acclimation and pH adaptation, and then treated without or with PEG (150 g l^{-1}) in the simplified nutrient solution (pH 4.5) for 24 h. Apoplastic proteins were extracted from root tips, separated by 2D-IEF/SDS-PAGE, and stained by CBB. Treatment-affected spots were marked by arrows and numbered consecutively. Three independent biological replications of each treatment were analysed using Image Master™ 2D PLATINUM Software 6.0. In (B), bars represent means ±SD, n=3. *, **, and *** denote significant PEG treatment differences at P<0.05, P<0.01, and P<0.001, respectively. (This figure is available in colour at *JXB* online.)

without SDS in the extraction buffer to be able to differentiate between hydrophilic and hydrophobic dehydrin. We found that dehydrin appeared predominantly in the water-soluble protein fraction (Fig. 6, lane A), whereas hardly any dehydrin was found in the water-insoluble protein fraction (Fig. 6, lane E). In addition, PEG treatment did not affect the protein abundance of dehydrin in root tips of bean (Fig. 6, lanes A and B), in agreement with the results of the 2D-IEF/SDS-PAGE of total and apoplastic protein separation (Figs 2 and 3). The two protein bands suggested the presence of two dehydrin isoforms.

Prediction of protein phosphorylation sites by using KinasePhos 2.0 software (http://kinasephos2.mbc.nctu.edu.tw/index.html; Wong *et al.*, 2007) revealed that dehydrin (GenBank accession no. AAB00554) contains 18 serine (S), seven threonine (T), and three tyrosine (Y) predicted potential phosphorylated sites (Supplementary Fig. S5 at *JXB* online).

Discussion

Physiological osmotic adjustment and modification of CW extensibility have been suggested as two major mechanisms involved in the maintenance of root elongation during water deficit (Sharp *et al.*, 2004; Yamaguchi and Sharp, 2010). In this study, functional categorization of total soluble proteins showed that the majority of the affected proteins were involved in primary metabolism (Supplementary Fig. S2, Table 1), particularly carbohydrate metabolism, confirming

Table 3. *List of 13 apoplastic proteins with significantly different abundance in the root tips of common bean genotype VAX 1 in response to PEG*

Plants were pre-cultured in a simplified nutrient solution containing 5 mM $CaCl_2$, 1 mM KCl, and 8 μM H_3BO_3 for 48 h for acclimation and pH adaptation, and then treated without or with PEG (150 g l^{-1}) in the simplified nutrient solution (pH 4.5). These 13 protein spots are shown in the CBB-stained 2D-IEF/SDS–PAGE gels of Figs 3 and Supplementary Fig. S3. Spot No. relate to the corresponding spot number in Fig. 3 and in supplemental Fig. S3. FC: fold change (the relative protein spot volume of +PEG treatment to the relative protein spot volume of -PEG treatment). The proteins were identified by nano LC-MS/MS and BLASTed in NCBI database. NI, not identified; MW, molecular weight. See Supplementary Table S1 at JXB online for further details.

Spot no.	Identity	MW (Da)	GenBank acc. no.	FC
1	NI	–	–	0.486
2	NI	–	–	0.607
3	Fructokinase (*Arachis hypogaea*)	20 047.7	ACF74294	0.636
4	Pathogenesis-related protein 1 (PvPR1) (*Phaseolus vulgaris*)	16 511.4	CAA43637	0.635
5	NI	–	–	0.616
6	Beta xylosidase (*Fragaria×ananassa*)	83 468.2	AAS17751	1.768
7	NI	–	–	2.067
8	NI	–	–	2.136
9	Pectinacetylesterase precursor (*Vigna radiata* var. Radiata)	43 804.9	CAA67728	1.730
10	Serine hydroxymethyltransferase, putative (*Ricinus communis*)	51 889.9	XP_002522806	1.935
11	Serine carboxypeptidase, putative (*Ricinus communis*)	50 034.7	XP_002521402	1.709
12	Serine hydroxymethyltransferase (*Gossypium hirsutum*)	51 889.9	ACJ11726	1.771
13	Fructose-1.6-bisphosphate aldolase (*Pisum sativum*)	38 473.4	CAA61947	1.692

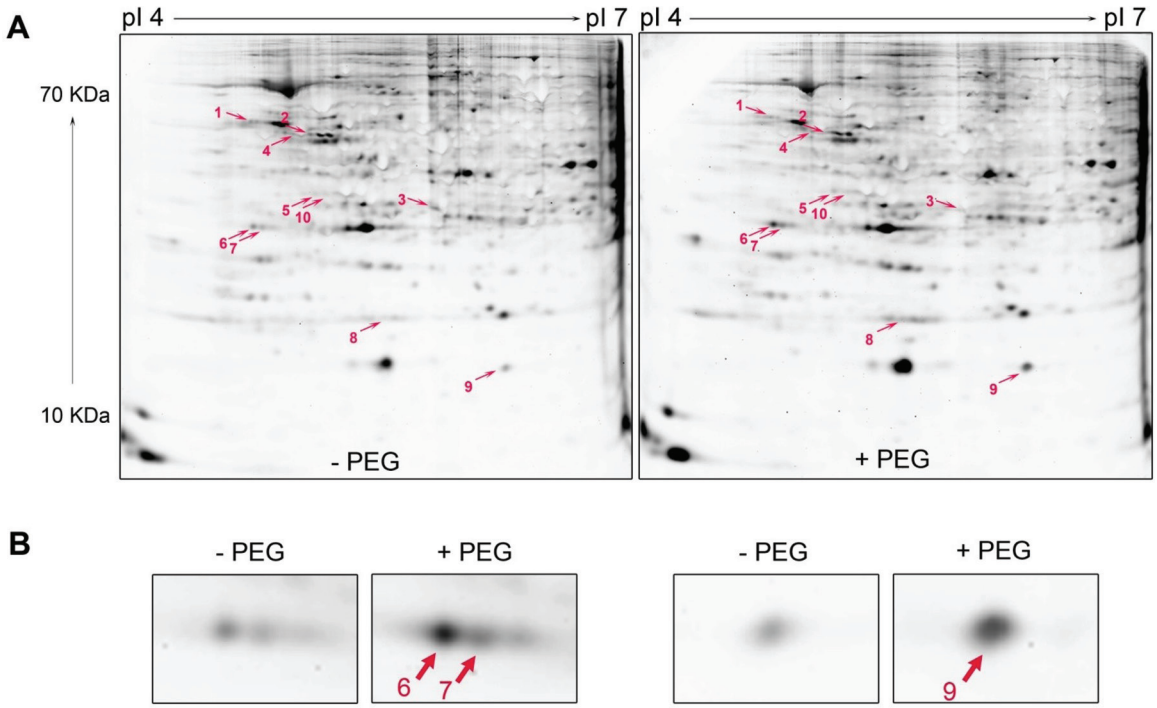

Fig. 4. Representative Pro-Q DPS-stained 2D-IEF/SDS-PAGE gels of the total soluble proteins in the control (–PEG) and PEG-treated root tips of common bean genotype VAX 1 (A) and three magnified spots with PEG treatment-enhanced protein abundance (B). Plants were pre-cultured in a simplified nutrient solution containing 5 mM $CaCl_2$, 1 mM KCl, and 8 μM H_3BO_3 for 48 h for acclimation and pH adaptation, and then treated without or with PEG (150 g l^{-1}) in the simplified nutrient solution (pH 4.5) for 24 h. Proteins were extracted from the root tips, separated by 2D-IEF/SDS-PAGE, and stained by Pro-Q DPS. Treatment-affected spots were marked by arrows and numbered consecutively. Three independent biological replications of each treatment were analysed using the Image Master™ 2D PLATINUM Software 6.0. (This figure is available in colour at *JXB* online.)

the important role of accumulation of carbohydrates and soluble amino acids involved in osmotic adjustment (Morgan, 1984). On the other hand, protein synthesis and modification of carbohydrates regulated by the proteins involved in metabolic pathways may facilitate the adjustment of CW synthesis and extensibility, and thus the regulation of root elongation.

Table 4. *List of 10 phosphoproteins with significantly different abundance in the root tips of common bean genotype VAX 1 in response to PEG*

Plants were pre-cultured in a simplified nutrient solution containing 5 mM $CaCl_2$, 1 mM KCl, and 8 μM H_3BO_3 for 48 h for acclimation and pH adaptation, then treated without or with PEG (150 g l^{-1}) in the simplified nutrient solution (pH 4.5). These 10 phosphoprotein spots are shown in the Pro-Q DPS-stained 2D-IEF/SDS–PAGE gels of Fig. 4 and in Supplementary Fig. S4. Spot no. relates to the corresponding spot number of Fig. 4 and Supplementary Fig. S4. FC, fold change (the relative protein spot volume of +PEG treatment to the relative protein spot volume of –PEG treatment). The proteins were identified by nano LC-MS/MS and BLASTed in NCBI database. See Supplementary Table S1 at JXB online for further details. MW, molecular weight.

Spot no.	Identity	MW (Da)	GenBank acc. no.	FC
1	Ser/Thr-specific protein phosphatase 2A A regulatory subunit β isoform (*Medicago sativa* subsp.×varia)	65161.6	AAG29594	0.647
2	Pyruvate kinase (*Lactuca sativa*)	56174.9	ABS87384	0.481
3	Branched-chain amino acid aminotransferase, putative (*Ricinus communis*)	45159.9	XP_002530599	0.541
4	Glucose-6-phosphate isomerase (*Zea mays*)	68403.5	NP_001147983	1.837
5	Actin (*Phaseolus acutifolius*)	33121.3	AAZ95077	2.277
6	Dehydrin (*Phaseolus vulgaris*)	22955.6	AAB00554	2.048
7	Dehydrin (*Phaseolus vulgaris*)	22955.6	AAB00554	1.846
8	Lactoylglutathione lyase, putative/glyoxalase I, putative (*Arabidopsis thaliana*)	20830.4	NP_001030996	2.414
9	Dehydrin (*Phaseolus vulgaris*)	22955.6	AAB00554	2.438
10	Dehydrin (*Phaseolus vulgaris*)	22955.6	AAB00554	1.625

Also, some proteins are supposed to play key roles in the protection against OS-induced severe physical destruction of CW integrity, such as dehydrin (Layton *et al.*, 2010), which was highly significantly changed in phosphorylation state by OS and localized in the CW in this study. Therefore, based on the above information, the discussion below will particularly focus on carbohydrate and amino acid metabolism and on CW-related proteins.

The osmotic adjustment in the growing root region in response to OS can in part result from increased net accumulation rates of osmotic solutes. Physiological factors influencing such accumulation rates are solute synthesis, uptake, catabolism, and utilization. All of these represent adaptive responses contributing to growth maintenance (Sharp *et al.*, 2004). It has been reported that OS increases sugar (e.g. fructose, glucose, and sucrose) accumulation in the roots of mung bean (*Vigna mungo*) seedlings (Itoh *et al.*, 1987) and the tropical tree *Colophospermum mopane* (Johnson *et al.*, 1996). Fructokinase specifically catalyses the transfer of a phosphate group from ATP to fructose, thereby activating this sugar for further metabolic processes. In this study, OS-induced reduced abundance of fructokinase in the root tips of common bean (Fig. 2, Supplementary Fig. S1, Table 1) may lead to fructose accumulation, and in this sense may be regarded as part of osmotic adjustment. Indeed, in soybean roots, Toorchi *et al.* (2009) also found by proteomic analysis that PEG-induced OS reduced the formation of a fructokinase 2 protein.

In *Arabidopsis*, Hummel *et al.* (2010) found that organic acids in addition to K^+ are main contributors to osmotic adjustment under water-deficit conditions. We previously reported that PEG-induced OS increased citrate, malate, *cis*-aconitate, and fumarate contents in root tips of common bean (Yang *et al.*, 2010), indicating a major role for the accumulation of these organic acids in osmotic adjustment. Isocitrate dehydrogenase is an enzyme that participates in the citric acid cycle. It catalyses oxidative decarboxylation of isocitrate to α-ketoglutarate and requires either NAD^+ or $NADP^+$ as co-substrate, producing NADH and NADPH, respectively. It was thought (Chen and Gadal, 1990) that citrate in the cytosol is first converted to isocitrate by the action of aconitase, and then to 2-oxoglutarate by the action of NADP-specific isocitrate dehydrogenase (NADP-ICDH). Subsequently, 2-oxoglutarate is utilized as carbon skeleton for the glutamine synthase/glutamate synthase pathway. Thus, a decrease in NADP-ICDH activity was associated with the accumulation of citrate in the plant tissue (Sadka *et al.*, 2000; Kihara *et al.*, 2003). In contrast, in the present study, it was found that OS increased the expression of NADPH-specific ICDH in root tips of common bean (Fig. 2, Supplementary Fig. S1, Table 1), thus not supporting the hypothesis that increased accumulation of citrate in the cytosol is a consequence of reduced NADP-ICDH activity (Massonneau *et al.*, 2001; Anoop *et al.*, 2003; Rangel *et al.*, 2010). However, on the other hand, enhanced formation of NADPH-specific ICDH due to OS may increase the accumulation of citrate in root tips through increasing citric acid cycle turnover. Moreover, it may be involved in defence processes, since NADP-ICDH was shown to play an important role in cellular defence against stress-induced oxidative injury (Jo *et al.*, 2002; Lee *et al.*, 2002). Liu *et al.* (2010) found that an isolated cDNA encoding cytosolic NADP-dependent ICDH from maize conferred salt tolerance to *Arabidopsis*.

Phosphoglycerate mutase (PGM) is a glycolytic enzyme, which catalyses the conversion of 3-phosphoglycerate to 2-phosphoglycerate. Ergen *et al.* (2009) found that the expression of the gene encoding PGM of wild durum wheat

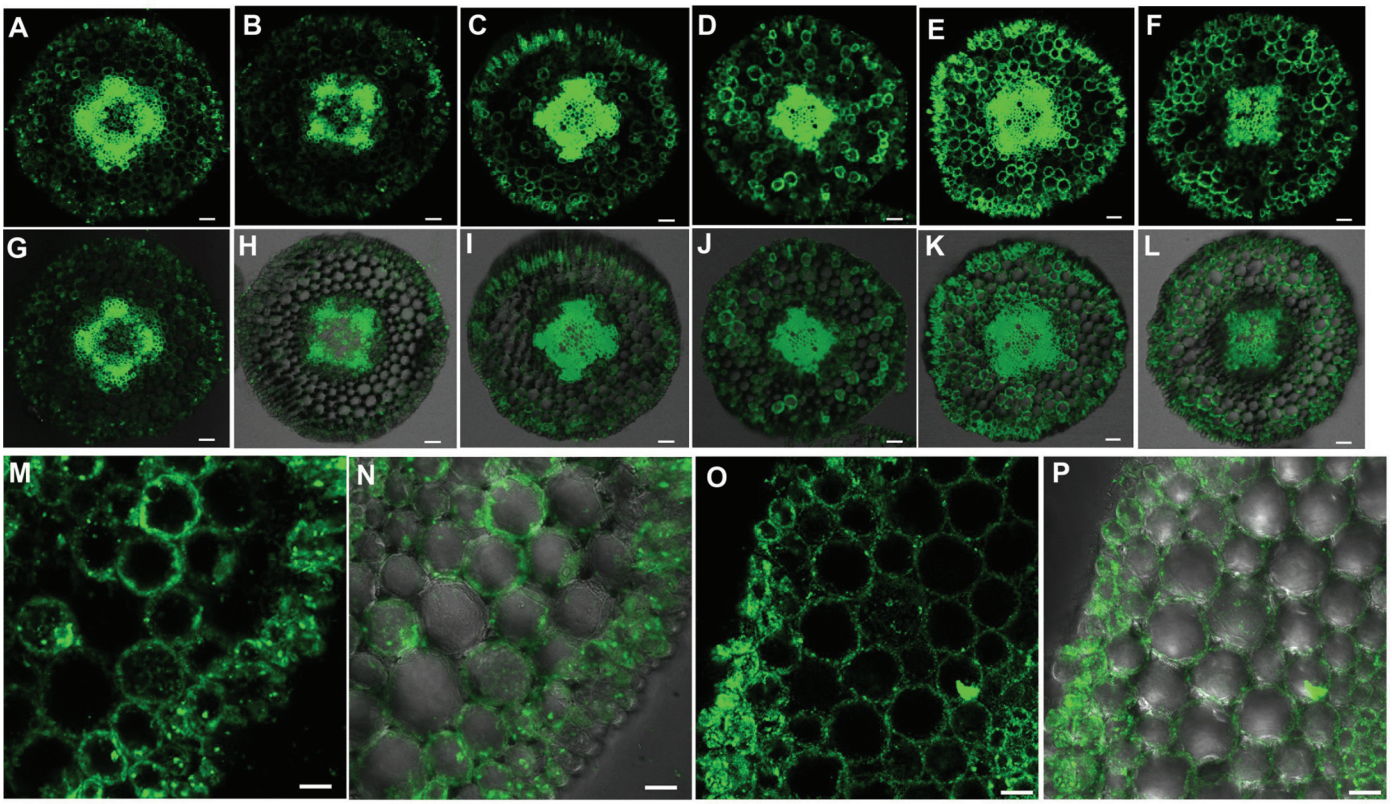

Fig. 5. Cellular immunolocalization of dehydrin in the root tips of common bean. Plants were pre-cultured in a simplified nutrient solution containing 5 mM $CaCl_2$, 1 mM KCl, and 8 μM H_3BO_3 for 48 h for acclimation and pH adaptation, and then treated without or with PEG (150 g l^{-1} PEG 6000) in the simplified nutrient solution (pH 4.5) for 24 h. Transverse root sections were treated with the anti-dehydrin polyclonal antibody and secondary anti-rabbit IgG–FITC. The images were captured with a confocal laser-scanning microscope (see Materials and methods). (A–F, M, O) Fluorescence of dehydrin; (G–L, N, P) merged image of dehydrin.(A, G, D, J) root apical 0–3 mm segments; (B, H, E, K) root apical 3–6 mm segments; (C, I, F, L) root apical 6–10 mm segments; (M, N) close-up of immunostaining of dehydrin in root apical 3–6 mm segments; (O, P) close-up of immunostaining of dehydrin in root apical 3–6 mm segments after plasmolysing the cells with 0.8 M manitol. (A–C, G–I) No PEG treatment (–PEG); (D–F, J–P) PEG treatment (+PEG). Bars, 50 μm (A–L); 20 μM (M–P).

(*Triticum turgidum*) was promoted in leaves while it was suppressed in roots during dehydration. Mazarei *et al.* (2003) observed that an *AtPGM* gene in *Arabidopsis* was localized in the shoot and root meristems, and that expression was downregulated by ABA. However, the function of this protein in stress responses remains to be elucidated. *Myo*-inositol 1-phosphate synthase (MIPS) catalyses the rate-limiting step in the synthesis of *myo*-inositol. It was reported that *mips1* mutants resulted in lowered *myo*-inositol levels and enhanced cell death in *Arabidopsis* (Meng *et al.*, 2009; Donahue *et al.*, 2010). Moreover, Donahue *et al.* (2010) provided evidence that *mips1* mutants had increased sensitivity to ABA and OS (salt and sorbitol treatment), which could be rescued by *myo*-inositol supplementation. The OS-induced suppression of MIPS in this study (Fig. 2, Supplementary Fig. S1, Table 1) suggests that the root tips of common bean suffered severe stress causing cell damage through lowered *myo*-inositol abundance. Enolase is responsible for the conversion of 2-phosphoglycerate to phosphoenolpyruvate, which is involved in glycolysis. Enolase was detected in the CWs of *Candida albicans*, *Arabidopsis thaliana*, *Medicago sativa*, and *Zea mays* (Chivasa *et al.*, 2002; Pitarch *et al.*, 2002; Watson *et al.*, 2004; Zhu *et al.*, 2006). Using immunolocalization, enolase was shown to be secreted to the CW or the extracellular space, even though it lacked a signal peptide (Edwards *et al.*, 1999). In this study, the abundance of enolase was enhanced by PEG treatment (Fig. 2, Supplementary Fig. S1, Table 1). The role of upregulation of enolase under OS remains unclear.

Some proteins involved in amino acid biosynthesis were differentially affected in abundance by OS in this study, such as *S*-adenosylmethionine synthase (methionine adenosyltransferase, SAMS), methionine synthase (MetS) and D-3-phosphoglycerate dehydrogenase (PHGDH) (Fig. 2, Supplementary Fig. S1, Table 1). MetS catalyses the final step in methionine biosynthesis and SAMS catalyses the conversion of ATP and methionine into *S*-adenosylmethionine (SAM) (Ravanel *et al.*, 1998). SAM serves as a co-factor in a variety of biochemical reactions in all living organisms. It acts as a methyl donor to proteins, lipids, polysaccharides, and nucleic acids (Tabor and Tabor 1984), participates in CW lignin synthesis (Sederoff and Chang 1991), and mediates the biosynthesis of ethylene (Yang and Hoffman, 1984; Kende 1993). Also, SAM is believed to play a regulatory role in the synthesis of methionine and other aspartate-derived

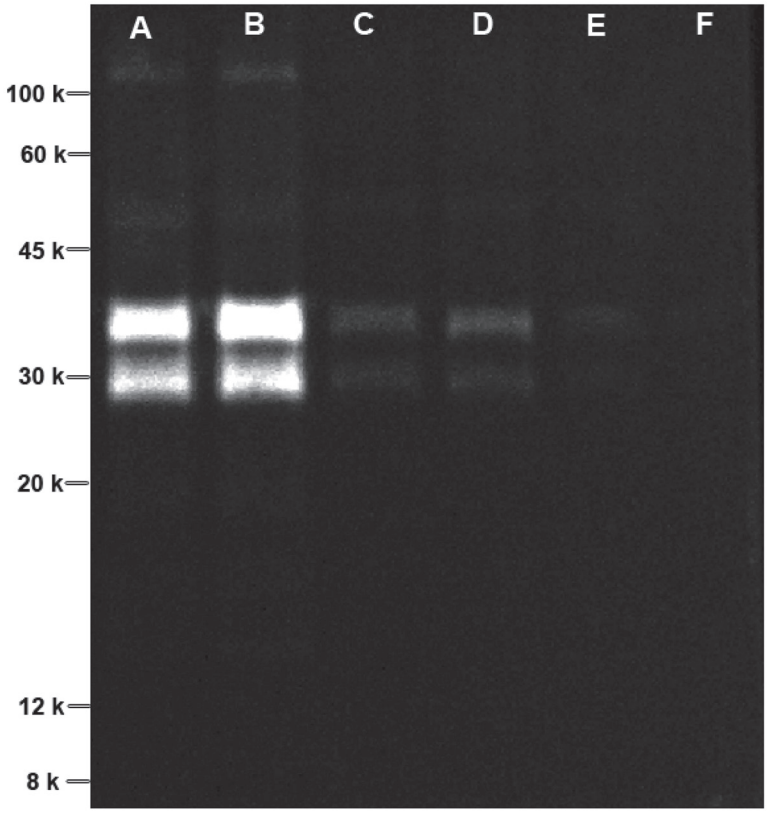

Fig. 6. Fluorescent western blotting of dehydrin protein in the root tips of common bean. Plants were pre-cultured in a simplified nutrient solution containing 5 mM $CaCl_2$, 1 mM KCl, and 8 μM H_3BO_3 for 48 h for acclimation and pH adaptation, and then treated without or with PEG (150 g l^{-1} PEG 6000) in the simplified nutrient solution (pH 4.5) for 24 h. The proteins from root tips treated without and with PEG were fractionally extracted with protein extraction buffer without and with 1% (w/v) SDS (see Materials and methods). Lanes: A, fraction I of –PEG; B, fraction I of +PEG; C, fraction II of –PEG; D, fraction II of +PEG; E, fraction III (+1% SDS) of –PEG; F, fraction III (+1% SDS) of +PEG.

amino acids (Peleman *et al.*, 1989). Manavella *et al.* (2006) demonstrated that overexpression of the sunflower (*Helianthus annuus*) HD-Zip protein subfamily 1 member *Hahb-4* transcription factor in *A. thaliana* improved desiccation tolerance via the repression of SAMS transcription and 1-aminocyclopropane-1-carboxylate oxidase, and subsequently suppressed the biosynthesis of ethylene. Ingram and Bartels (1996) reported that drought-caused alterations in the chemical composition and physical properties of the CW (e.g. CW extensibility) may involve genes encoding SAMS. Under non-stressed conditions, higher expression of *SAMS* genes correlated with the extent of lignification of tissues in *Arabidopsis* (Peleman *et al.*, 1989). Lignification of CW by methylation of lignin monomers was described as one mechanism to avoid water loss under dehydration (Bhushan *et al.*, 2007). Indeed, it has been reported that water deficit intensified the lignifications of root tip CWs in maize (Fan *et al.*, 2006) and soybean (Yamaguchi *et al.*, 2010). Moreover, it has been suggested that cellular levels of SAM are regulated by MetS activity forming methionine, a precursor of SAM (Ravanel *et al.*, 1998). Therefore, the induction of MetS transcripts suggests an increased production of methionine and lignin methylation by SAM. Recent results confirmed that SAMS was involved in tolerance to abiotic stresses such as salinity (Sanchez-Aguayo *et al.*, 2004; Jiang *et al.*, 2007) and drought stress (Toorchi *et al.*, 2009; Pandey *et al.*, 2010). In this study, PEG treatment led to increased abundance of a MetS (spot 21 in Fig. 2, Supplementary Fig. S1, Table 1) and SAMS (spot 20 in Fig. 2, Supplementary Fig. S1, Table 1), while the amount of a further three SAMS proteins (spots 1, 2, and 3 in Fig. 2, Supplementary Fig. S1, Table 1) in the root tips were repressed. The PEG-induced differential regulation of SAMS proteins may be indicative of different isoforms of this protein. Under OS conditions, the increase in SAMS may either improve lignification of root tip CWs or increase biosynthesis of ethylene, while downregulation of SAMS may be caused by a changed demand for more methyl groups for lignin methylation (Bhushan *et al.*, 2007). It is known that transcriptional and translational levels of SAMS are downregulated by OS (Seki *et al.*, 2002; Yan *et al.*, 2005; Jiang *et al.*, 2007; Toorchi *et al.*, 2009).

Sharp *et al.* (2004) suggested that, in maize, the extent of osmotic adjustment in the primary root tip, although substantial, was insufficient in roots growing under severe drought to maintain turgor comparable to well-watered levels. This was assessed directly by measuring the spatial distribution of turgor using a cell-pressure probe, which showed that turgor was reduced by >50% throughout the root-elongation zone

of roots growing at a water potential of –1.6 MPa compared with well-watered control plants (Spollen and Sharp, 1991). Thus, enhancement of CW extensibility may contribute to the maintenance of root elongation in the apical region of water-stressed roots (Sharp *et al.*, 2004; Yamaguchi and Sharp, 2010). Under multiple abiotic stress conditions, we recently found that OS-induced reduction of CW porosity could improve Al resistance by restricting Al accumulation in the apoplast of common bean root tips (Yang *et al.*, 2010). Also, by means of a transcriptome analysis, we identified some genes encoding proteins involved in CW modification (xyloglucan endotransglucosylase/hydrolase, XTH) and CW structure (HRGPs), which were supposed to play major roles in the PEG-mediated decrease of CW porosity (Yang *et al.*, 2011). Several CW proteins/enzymes are believed to play roles in modifying the CW structure and controlling CW extension. These include expansin, XTH, and glucanases (Wu and Cosgrove, 2000; Bray, 2004; Sharp *et al.*, 2004; Moore *et al.*, 2008). Therefore, we aimed at identifying these proteins and clarifying their response to PEG treatment by extracting apoplastic and loosely ionically bound proteins in root tips of common bean and separating them by protein electrophoresis techniques. Unlike what we expected, only a low protein yield was obtained by a fractional infiltration method. In addition, the extracted apoplastic protein yield in each infiltration step was reduced in PEG-treated roots (Table 2), further supporting the suggestion that PEG-induced OS reduces CW porosity (Yang *et al.*, 2010), thereby reducing exchangeability of these proteins by extractants. Thus, proteins with a high molecular weight could not be exchanged so that predominantly small molecular proteins were identified in this study. Although Zhu *et al.* (2007) identified a large number of water deficit-induced CW proteins in maize using the same extraction procedures employed in the current study, the type I CW of common bean is different from the type II CW of maize: the former contains higher pectic polysaccharides (Carpita and Gibeaut, 1993), which is the main factor determining CW porosity (Baron-Epel *et al.*, 1988).

In spite of this, 13 PEG-induced differentially affected proteins in the CW were obtained and eight were identified by MS analysis (Fig. 3, Table 3). TOS-induced reduction of fructokinase was also found in the CW fraction. It has been suggested that fructose formed from sucrose cleavage could be directly and rapidly converted into UDP-glucose via the hexose-phosphate pool (i.e. fructose-6-phosphate↔glucose-6-phosphate↔glucose-1- phosphate), and subsequently transferred to the apoplast for synthesis of CW polysaccharides (Konishi *et al.*, 2004). Thus, it appears that a decrease in fructokinase may result in a reduction in CW polysaccharide content in root tips, impeding root growth under OS, since fructokinase catalyses the transfer of fructose into fuctose-6-phosphate. Toorchi *et al.* (2009) also reached a similar conclusion. Indeed, Odanaka *et al.* (2002) reported that suppression of the gene *Frk2* encoding fructose kinase inhibited root growth of tomato. In conclusion, fructokinase may play a role in the regulation of the energy metabolism: (i) by providing fructose-6-phosphate for glycolysis; and/or (ii) through conversion to UDP-glucose to support biosynthesis of CW material (Karni and Aarni, 2002).

Fructose-1,6-bisphosphate aldolase reversibly catalyses the conversion of fructose-1,6-bisphosphate to glyceraldehyde-3-phosphate. The extracellular matrix proteome analysis revealed that fructose-1,6-bisphosphate aldolase was indeed a CW protein, which was increased during dehydration stress in chickpea (*Cicer arietinum*) (Bhushan *et al.*, 2007) and rice (*Oryza sativa*) (Pandey *et al.*, 2010), corroborating the results of this study showing that PEG-induced apoplastic dehydration increased the abundance of apoplastically localized fructose-1,6-bisphosphate aldolase in the root tips of common bean (Fig. 3, Table 3). Enhanced synthesis of fructose-1,6-bisphosphate aldolase was also reported as a response to salt stress in rice (Abbasi and Komatsu 2004) and the mangrove plant *Bruguiera gymnorhiza* (Tada and Kashimura, 2009). Enhanced formation of fructose-1,6-bisphosphate aldolase may increase the flow of carbon through the Calvin cycle and lead to C-skeleton production for subsequent increased carbon flux through glycolysis. These traits would also lead to osmolyte production and contribute to OS tolerance.

Pathogenesis-related proteins (PRs) are mainly involved in the defence against pathogenic constraints and in general adaptation to stressful environments. The CW is the major accumulation site of these PRs (Edreva, 2005). To our knowledge, the biochemical function of PR1 is not fully known. However, suppression of PR1 by OS (Fig. 3, Table 3) in this study may reflect a lower protection level and severe root-cell damage. β-Xylosidase was found in the stock of pathogen-degrading enzymes (Tezuka *et al.*, 1993). A gene, *AtBLX1*, encoding β-xylosidase in *Arabidopsis* was proposed to be involved in secondary CW hemicellulose metabolism and plant development (Goujon *et al.*, 2003). In contrast to our results showing PEG-mediated increased abundance of β-xylosidase in the CW of bean root tips (Fig. 3, Table 3), Zhu *et al.* (2007) found that water deficit reduced β-xylosidase in the apical 3–7 mm region of the maize primary roots. The exact function of β-xylosidase in response to osmotic/drought stress remains to be elucidated. In addition, the amount of pectin acetylesterase, serine hydroxymethyltransferase, and serine carboxypeptidase was enhanced by OS, but the role of these in OS is not yet known.

Phosphoproteomics revealed that three proteins showed reduced and seven proteins increased phosphorylation by OS. Of these, dehydrin underwent significantly enhanced phosphorylation by OS (Fig. 4, Table 4), while no PEG effect on abundance of dehydrin by CBB staining (data not shown) and western blotting (Fig. 6) was found, indicating that the activation of dehydrin during OS by phosphorylation may play an important role in root responses to OS. Dehydrins are the second biggest group of late embryogenesis abundant proteins, which are well known to play crucial roles in cellular dehydration tolerance (Ingram and Bartels, 1996; Hundertmark and Hincha, 2008) and desiccation tolerance of angiosperm plants (Gaff and Oliver, 2013). A number of studies have demonstrated that dehydrin proteins play an important role in drought tolerance by preventing membrane denaturation and maintaining the integrity of the CW (Lopez *et al.*, 2003;

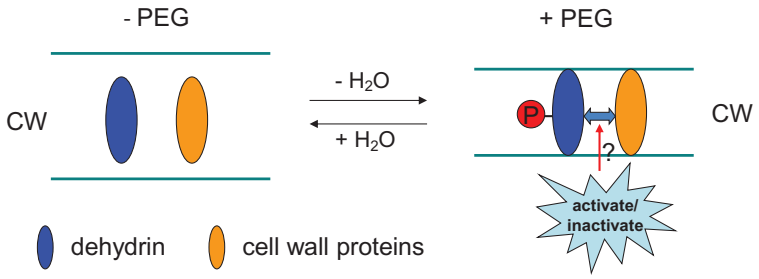

Fig. 7. Schematic model of the potential interaction between phosphorylated dehydrin protein and other CW proteins under OS. (This figure is available in colour at *JXB* online.)

Collett *et al.*, 2004; Vicré *et al.*, 2004; Samarah *et al.*, 2006; Hu *et al.*, 2010). Dehydrins are known to undergo phosphorylation both *in vivo* and *in vitro* (Heyen *et al.*, 2002; Jiang and Wang, 2004; Alsheikh *et al.*, 2005; Brini *et al.*, 2006; Röhrig *et al.*, 2006).

Dehydrins were found to be localized in various subcellular sites including the plasma membrane, cytoplasm, and nucleus (Danyluk *et al.*, 1998; Wisniewski *et al.*, 1999; Carjuzaa *et al.*, 2008). Recently, Layton *et al.* (2010) observed that dehydrin accumulated mainly near the CW of dried tissues in the desiccation-tolerant fern *Polypodium polypodioides*. The author supposed that the ability to avoid CW damage in some desiccation-tolerant species may be partially attributed to CW localization of dehydrins enabling reversible CW deformation. The cellular localization of dehydrin in CW was further verified by the present study (Fig. 5, Fig. 6). Dehydrins are extremely hydrophilic proteins (Close *et al.*, 1989), which can attract, sequester, and localize water, and may behave as a lubricant between either the plant CW and cell membrane or between individual CW layers. It has been reported that dehydrins are highly specialized proteins that lack a fixed three-dimensional structure and have evolved to maintain their disordered character under conditions such as water deficit, in which unfolded states of several globular proteins would tend to collapse (Mouillon *et al.*, 2008). However, the effect of phosphorylation on dehydrin structure is small and does not significantly enhance the response to OS induced by glycerol and PEG 4000 *in vitro* (Mouillon *et al.*, 2008). In spite of this, the studies *in vitro* may not reflect the response of dehydrin structure to phosphorylation *in vivo*, since dehydrins may interact with other proteins *in vivo*. In addition, the site of OS induced by glycerol and PEG 4000 is different from PEG 6000 because of the differences in molecular weight; the former solutes mainly induce OS in the cytoplasm, while the latter act additionally in the apoplast (Yang *et al.*, 2010). Thus, it appears that the increased dehydrin formation could play an important role in the protection of CW against breakage and in the maintenance of the mechanical CW integrity. Our previous study (Yang *et al.*, 2010) suggested that CW porosity was reduced by PEG-induced OS and quickly recovered after the removal of OS in root tips of common bean, which was concluded on the basis of the penetration of ions with a different hydrated ionic radius (Al^{3+}>La^{3+}>Sr^{2+}>Rb^{+}) into the apoplast, and CW modification proteins XTH, BEG, and the structural protein HRGP may participate in this reversible regulation (Yang *et al.*, 2011). Therefore, the phosphorylated dehydrins may prevent the CW from PEG-caused mechanical disruption by interacting with other CW proteins or may act independently, and consequently maintain the elastic extension (reversible stretching) properties of the CW and thus allow quick reversion of CW extension after removal of OS, as depicted in Fig. 7.

In conclusion, our large-scale proteomic analysis revealed the importance of carbohydrate and amino acid metabolism in the response of root tips to OS. Phosphoproteomics provided novel insights into the potential role of dehydrin as a CW structure modulator, which may participate in alteration of CW porosity by maintaining the integrity and reversible extension properties of the CW during OS.

Supplementary data

Supplementary data are available at *JXB* online.

Supplementary Fig. S1. Close-ups of significantly decreased and increased total soluble protein spots in response to PEG in the root tips of common bean genotype VAX 1.

Supplementary Fig. S2. Functional categories of the 22 significantly decreased and increased proteins in response to PEG-induced OS in the root tips of common bean genotype VAX 1.

Supplementary Fig. S3. Close-ups of significantly decreased and increased apoplastic protein spots in response to PEG in the root tips of common bean genotype VAX 1.

Supplementary Fig. S4. Close-ups and the relative volume of significantly decreased and increased phosphorylated protein spots in response to PEG in the root tips of common bean genotype VAX 1.

Supplementary Fig. S5. Prediction of potential phosphorylation sites of the dehydrin protein.

Supplementary Table S1. Detailed information for identified proteins including 22 total soluble proteins, 13 apoplastic proteins and 10 phosphorylated proteins, which are listed in Tables 1, 3 and 4, respectively, by nano LC-MS/MS.

Acknowledgements

This research was supported by a restricted core project from the Bundesministerium für Wirtschaftliche Zusammenarbeit/ Gesellschaft für Technische Zusammenarbeit (BMZ/GTZ)

(no. 05.7860.9-001.00) granted to the International Center for Tropical Agriculture (CIAT). We thank Dr Steve Beebe, Leader of the Bean Program of CIAT, for the supply of seeds of the common bean genotype.

References

Abbasi FM, Komatsu S. 2004. A proteomic approach to analyze salt-responsive proteins in rice leaf sheath. *Proteomics* **4,** 2072–2081.

Agrawal GK, Thelen JJ. 2009. A high-resolution two dimensional gel- and Pro-Q DPS-based proteomics workflow for phosphoprotein identification and quantitative profiling. *Methods in Molecular Biology* **527,** 3–19.

Alsheikh MK, Svensson JT, Randall SK. 2005. Phosphorylation regulated ion-binding is a property shared by the acidic subclass dehydrins. *Plant, Cell and Environment* **28,** 1114–1122.

Anoop VM, Basu U, McCammon MT, McAlister HL, Taylor GJ. 2003. Modulation of citrate metabolism alters aluminum tolerance in yeast and transgenic canola overexpressing a mitochondrial citrate synthase. *Plant Physiology* **132,** 2205–2217.

Baron-Epel O, Gharyal PK, Schindler M. 1988. Pectins as mediators of wall porosity in soybean cells. *Planta* **175,** 389–395.

Beebe SE. 2012. Common bean breeding in the tropics. *Plant Breeding Reviews* **36,** 357–426.

Beebe S, Rao IM, Cajiao C, Grajales M. 2008. Selection for drought resistance in common bean also improves yield in phosphorus limited and favourable environments. *Crop Science* **48,** 582–592.

Bergmeyer HU, Bernt E. 1974. Malate dehydrogenase. In: Bergmeyer HU, ed. *Methoden der enzymatischen Analyse*, Band I. Weinheim: Verlag Chemie, 649–653.

Bhushan D, Pandey A, Choudhary MK, Datta A, Chakraborty S, Chakraborty N. 2007. Comparative proteomics analysis of differentially expressed proteins in chickpea extracellular matrix during dehydration stress. *Molecular and Cellular Proteomics* **6,** 1868–1884.

Bradford MM. 1976. A rapid and sensitive method for the quantitation of microgram quantities of protein utilizing the principle of protein-dye binding. *Analytical Biochemistry* **72,** 248–254.

Bray EA. 2004. Genes commonly regulated by water-deficit stress in *Arabidopsis thaliana*. *Journal of Experimental Botany* **55,** 2331–2341.

Brini F, Hanin M, Lumbreras V, Irar S, Pages M, Masmoudi K. 2006. Functional characterization of DHN-5, a dehydrin showing a differential phosphorylation pattern in two Tunisian durum wheat (*Triticum durum* Desf.) varieties with marked difference in salt and drought tolerance. *Plant Science* **172,** 20–28.

Carjuzaa P, Castellión M, Distéfano AJ, del Vas M, Maldonado S. 2008. Detection and subcellular localization of dehydrin-like proteins in quinoa (*Chenopodium quinoa* Willd.) embryos. *Protoplasma* **233,** 149–156.

Carpita NC, Gibeaut DM. 1993. Structural models of primary cell walls in flowering plants: consistency of molecular structure with the physical properties of the walls during growth. *The Plant Journal* **3,** 1–30.

Chen RD, Gadal P. 1990. Do the mitochondria provide the 2-oxoglutarate needed for glutamate synthesis in higher plant chloroplasts? *Plant Physiology and Biochemistry* **28,** 141–145.

Chivasa S, Ndimba BK, Simon WJ, Robertson D, Yu XL, Knox JP, Bolwell P, Slabas AR. 2002. Proteomic analysis of the *Arabidopsis thaliana* cell wall. *Electrophoresis* **23,** 1754–1765.

Close TJ, Kortt AA, Chandler PM. 1989. A cDNA-based comparison of dehydration-induced proteins (dehydrins) in barley and corn. *Plant Molecular Biology* **13,** 95–108.

Collett H, Shen A, Gardner M, Farrant JM, Denby KJ, Illing N. 2004. Towards transcript profiling of desiccation tolerance in *Xerophyta humilis*: construction of a normalized 11 k *X. humilis* cDNA set and microarray expression analysis of 424 cDNAs in response to dehydration. *Physiologia Plantarum* **122,** 39–53.

Danyluk J, Perron A, Houde M, Limin A, Fowler B, Benhamou N, Sarhan F. 1998. Accumulation of an acidic dehydrin in the vicinity of the plasma membrane during cold acclimation of wheat. *Plant Cell* **10,** 623–638.

Donahue JL, Alford SR, Torabinejad J, *et al.* 2010. The *Arabidopsis thaliana myo-inositol 1-phosphate synthase1* gene is required for myo-inositol synthesis and suppression of cell death. *Plant Cell* **22,** 888–903.

Edreva A. 2005. Pathogenesis-related proteins: research progress in the last 15 years. *General and Applied Plant Physiology* **31,** 105–124.

Edwards SR, Braley R, Chaffin WL. 1999. Enolase is present in the cell wall of *Saccharomyces cerevisiae*. *FEMS Microbiology Letters* **177,** 211–216.

Elias JE, Gygi SP. 2007. Target-decoy search strategy for increased confidence in large-scale protein identifications by mass spectrometry. *Nature Methods* **4,** 207–214.

Ergen NZ, Thimmapuram J, Bohnert HJ, Budak H. 2009. Transcriptome pathways unique to dehydration tolerant relatives of modern wheat. *Functional and Integrative Genomics* **9,** 377–396.

Fan L, Linker R, Gepstein S, Tanimoto E, Yamamoto R, Neumann PM. 2006. Progressive inhibition by water deficit of cell wall extensibility and growth along the elongation zone of maize roots is related to increased lignin metabolism and progressive stelar accumulation of wall phenolics. *Plant Physiology* **140,** 603–612.

Fan L, Neumann PM. 2004. The spatially variable inhibition by water deficit of maize root growth correlates with altered profiles of proton flux and cell wall pH. *Plant Physiology* **135,** 2291–2300.

Führs H, Hartwig M, Molina LE, Heintz D, Van Dorsselaer A, Braun HP, Horst WJ. 2008. Early manganese-toxicity response in *Vigna unguiculata* L.—a proteomic and transcriptomic study. *Proteomics* **8,** 149–159.

Gaff DF, Oliver M. 2013. The evolution of desiccation tolerance in angiosperm plants: a rare yet common phenomenon. *Functional Plant Biology* **40,** 315–328.

Goujon T, Minic Z, El Amrani A, Lerouxel O, Aletti E, Lapierre C, Joseleau JP, Jouanin L. 2003. *AtBXL1*, a novel higher plant (*Arabidopsis thaliana*) putative β-xylosidase gene, is involved in secondary cell wall metabolism and plant development. *The Plant Journal* **33,** 677–690.

Graham PH. 1978. Some problems and potentials of field beans (*Phaseolus vulgaris* L.) in Latin America. *Field Crops Research* **1,** 295–317.

Graham PH, Ranalli P. 1997. Common bean (*Phaseolus vulgaris* L.). *Field Crops Research* **53,** 131–146.

Heyen BJ, Alsheikh MK, Smith EA, Torvik CF, Seals DF, Randall SK. 2002. The calcium-binding activity of a vacuole-associated, dehydrin-like protein is regulated by phosphorylation. *Plant Physiology* **130,** 675–687.

Hu L, Wang Z, Du H, Huang B. 2010. Differential accumulation of dehydrins in response to water stress for hybrid and common bermudagrass genotypes differing in drought tolerance. *Journal of Plant Physiology* **167,** 103–109.

Hummel I, Pantin F, Sulpice R, *et al.* 2010. Arabidopsis plants acclimate to water deficit at low cost through changes of carbon usage: an integrated perspective using growth, metabolite, enzyme, and gene expression analysis. *Plant Physiology* **154,** 357–372.

Hundertmark M, Hincha DK. 2008. LEA (late embryogenesis abundant) proteins and their encoding genes in *Arabidopsis thaliana*. *BMC Genomics* **9,** 118.

Ingram J, Bartels D. 1996. The molecular basis of dehydration tolerance in plants. *Annual Review of Plant Physiology and Plant Molecular Biology* **47,** 377–403.

Ishitani M, Rao I, Wenzl P, Beebe S, Tohme J. 2004. Integration of genomics approach with traditional breeding towards improving abiotic stress adaptation: drought and aluminum toxicity as case studies. *Field Crops Research* **90,** 35–45.

Itoh K, Nakahara K, Ishikawa H, Ohta E, Sakata M. 1987. Osmotic adjustment and osmotic constituents in roots of mung bean seedlings. *Plant and Cell Physiology* **28,** 397–403.

Jensen O. 2004. Modification-specific proteomics: characterization of post-translational modifications by mass spectrometry. *Current Opinion in Chemical Biology* **8,** 33–41.

Jiang X, Wang Y. 2004. Beta-elimination coupled with tandem mass spectrometry for the identification of in vivo and in vitro phosphorylation sites in maize dehydrin DHN1 protein. *Biochemistry* **43,** 15567–15576.

Jiang Y, Yang B, Harris NS, Deyholos MK. 2007. Comparative proteomic analysis of NaCl stress-responsive proteins in Arabidopsis roots. *Journal of Experimental Botany* **58,** 3591–3607.

Jo SH, Lee SH, Chun HS, Lee SM, Koh HJ, Lee SE, Chun JS, Park JW, Hun TL. 2002. Cellular defence against UVB-induced phototoxicity by cytosolic NADP-dependent isocitrate dehydrogenase. *Biochemical and Biophysical Research Communications* **292,** 542–549.

Johnson JM, Pritchard J, Gorham J, Tomos AD. 1996. Growth, water relations and solute accumulation in osmotically stressed seedlings of the tropical tree *Colophospermum mopane*. *Tree Physiology* **16,** 713–718.

Karni L, Aarni B. 2002. Fructokinase and hexokinase from pollen grains of bell pepper (*Capsicum annuum* L.): possible role in pollen germination under conditions of high temperature and CO_2 enrichment. *Annals of Botany* **90,** 607–612.

Kende H. 1993. Ethylene biosynthesis. *Annual Review of Plant Physiology and Plant Molecular Biology* **44,** 283–307.

Kihara T, Ohno T, Koyama H, Sawafuji T, Hara T. 2003. Characterization of NADP-isocitrate dehydrogenase expression in a carrot mutant cell line with enhanced citrate excretion. *Plant and Soil* **248,** 145–153.

Konishi T, Ohmiya Y, Hayashi T. 2004. Evidence that sucrose loaded into the phloem of a poplar leaf is used directly by sucrose synthase associated with various β-glucan synthases in the stem. *Plant Physiology* **134,** 1146–1152.

Layton BE, Boyd MB, Tripepi MS, Bitonti BM, Dollahon MNR, Balsamo RA. 2010. Dehydration-induced expression of a 31-kDa dehydrin in *Polypodium polypodioides* (Polypodiaceae) may enable large, reversible deformation of cell walls. *American Journal of Botany* **97,** 535–544.

Lee SM, Koh HJ, Park DC, Song BJ, Huh TL, Park JW. 2002. Cytosolic NADP-dependent isocitrate dehydrogenase status modulates oxidative damage to cells. *Free Radical Biology and Medicine* **32,** 1185–1196.

Liu Y, Shi Y, Song Y, Wang T, Li Y. 2010. Characterization of a stress-induced NADP-isocitrate dehydrogenase gene in maize confers salt tolerance in Arabidopsis. *Journal of Plant Biology* **53,** 107–112.

Livak KJ, Schmittgen TD. 2001. Analysis of relative gene expression data using real-time quantitative PCR and the $2^{-\Delta\Delta CT}$ method. *Methods* **25,** 402–408.

Lopez CG, Banowetz GM, Peterson CJ, Kronstad WE. 2003. Dehydrin expression and drought tolerance in seven wheat cultivars. *Crop Science* **43,** 577–582.

Manavella PA, Arce AL, Dezar CA, Bitton F, Renou JP, Crespi M, Chan RL. 2006. Cross-talk between ethylene and drought signalling pathways is mediated by the sunflower Hahb-4 transcription factor. *The Plant Journal* **48,** 125–137.

Massonneau AS, Langlade N, Leon S, Smutny J, Vogt E, Neumann G, Martinoia E. 2001. Metabolic changes associated with cluster root development in white lupin (*Lupinus albus* L.): relationship between organic acid excretion, sucrose metabolism and energy status. *Planta* **213,** 534–542.

Mazarei M, Lennon KA, Puthoff DP, Rodermel SR, Baum TJ. 2003. Expression of an Arabidopsis phosphoglycerate mutase homologue is localized to apical meristems, regulated by hormones, and induced by sedentary plant-parasitic nematodes. *Plant Molecular Biology* **53,** 513–530.

Meng PH, Raynaud C, Tcherkez G, *et al.* 2009. Crosstalks between myo-inositol metabolism, programmed cell death and basal immunity in Arabidopsis. *PLoS One* **4,** e7364.

Moore JP, Vicré-Gibouin M, Farrant JM, Driouich A. 2008. Adaptations of higher plant cell walls to water loss: drought vs desiccation. *Physiologia Plantarum* **134,** 237–245.

Morgan JM. 1984. Osmoregulation and water stress in higher plants. *Annual Review of Plant Physiology* **35,** 299–319.

Mouillon JM, Eriksson SK, Harryson P. 2008. Mimicking the plant cell interior under water stress by macromolecular crowding: disordered dehydrin proteins are highly resistant to structural collapse. *Plant Physiology* **148,** 1925–1937.

Neuhoff V, Stamm R, Eibl H. 1985. Clear background and highly sensitive protein staining with Coomassie Blue dyes in polyacrylamide gels: a systematic analysis. *Electrophoresis* **6,** 427–448.

Neuhoff V, Stamm R, Pardowitz I, Arold N, Ehrhardt W, Taube D. 1990. Essential problems in quantification of proteins following colloidal staining with Coomassie brilliant blue dyes in polyacrylamide gels, and their solution. *Electrophoresis* **11,** 101–117.

Nobel PS. 1991. *Physicochemical environmental plant physiology*. New York: Academic Press.

Odanaka S, Bennett AB, Kanayama Y. 2002. Distinct physiological roles of fructokinase isozymes revealed by gene-specific suppression of *Frk1* and *Frk2* expression in tomato. *Plant Physiology* **129,** 1119–1126.

Pandey A, Rajamani U, Verma J, Subba P, Chakraborty N, Datta A, Chakraborty S, Chakraborty N. 2010. Identification of extracellular matrix proteins of rice (*Oryza sativa* L.) involved in dehydration-responsive network: a proteomic approach. *Journal of Proteome Research* **9,** 3443–3464.

Peleman J, Boerjan W, Engler G, Seurinck J, Botterman J, Alliotte T, Van Montagu M, Inzé D. 1989. Strong cellular preference in the expression of a housekeeping gene of *Arabidopsis thaliana* encoding *S*-adenosylmethionine synthetase. *Plant Cell* **1,** 81–93.

Pitarch A, Sanchez M, Nombela C, Gil C. 2002. Sequential fractionation and two-dimensional analysis unravels the complexity of the dimorphic fungi *Candida albicans* cell wall proteome. *Molecular and Cellular Proteomicss* **1,** 967–982.

Poroyko V, Spollen WG, Hejlek LG, Hernandez AG, LeNoble ME, Davis G, Nguyen HT, Springer GK, Sharp RE, Bohnert HJ. 2007. Comparing regional transcript profiles from maize primary roots under well-watered and low water potential conditions. *Journal of Experimental Botany* **58,** 279–289.

Rangel AF, Rao IM, Braun H-P, Horst WJ. 2010. Aluminium resistance in common bean (*Phaseolus vulgaris*) involves induction and maintenance of citrate exudation from root apices. *Physiologia Plantarum* **138,** 176–190.

Rangel AF, Rao IM, Horst WJ. 2007. Spatial aluminium sensitivity of root apices of two common bean (*Phaseolus vulgaris* L.) genotypes with contrasting aluminium resistance. *Journal of Experimental Botany* **58,** 3895–3904.

Rao IM. 2001. Role of physiology in improving crop adaptation to abiotic stresses in the tropics: the case of common bean and tropical forages. In: Pessarakli M, ed. *Handbook of plant and crop physiology*, New York: Marcel Dekker, 583–613.

Ravanel S, Gakière B, Job D, Douce R. 1998. The specific features of methionine biosynthesis and metabolism in plants. *Proceedings of the National Academy of Sciences, USA* **95,** 7805–7812.

Röhrig H, Schmidt J, Colby T, Brautigam A, Hufnagel P, Bartels D. 2006. Desiccation of the resurrection plant *Craterostigma plantagineum* induces dynamic changes in protein phosphorylation. *Plant, Cell and Environment* **29,** 1606–1617.

Rose JKC, Bashir S, Giovannoni JJ, Jahn MM, Saravanan RS. 2004. Tackling the plant proteome: practical approaches, hurdles and experimental tools. *The Plant Journal* **39,** 715–733.

Sadka A, Dahan E, Or E and Cohen L. 2000. $NADP^+$-isocitrate dehydrogenase gene expression and isozyme activity during citrus fruit development. *Plant Science* **158,** 173–181.

Samarah NH, Mullen RE, Cianzio SR, Scott P. 2006. Dehydrin-like proteins in soybean seeds in response to drought stress during seed filling. *Crop Science* **46,** 2141–2150.

Sanchez-Aguayo I, Rodriguez-Galan JM, Garcia R, Torreblanca J, Pardo JM. 2004. Salt stress enhances xylem development and expression of *S*-adenosyl-L-methionine synthase in lignifying tissues of tomato plants. *Planta* **220,** 278–285.

Schägger H, von Jagow G. 1987. Tricine-sodium dodecyl sulfate-polyacrylamide gel electrophoresis for the separation of proteins in the range from 1 to 100 kDa. *Analytical Biochemistry* **166,** 368–379.

Sederoff R, Chang HM. 1991. Lignin biosynthesis. In: Lewin M, Goldstein IS, eds. *Wood structure and composition* . New York: Marcel Dekker, 263–285.

Seki M, Narusaka M, Ishida J, *et al.* 2002. Monitoring the expression profiles of 7000 Arabidopsis genes under drought, cold, and high-salinity stresses using a full-length cDNA microarray. *The Plant Journal* **31,** 279–292.

Serraj R, Sinclair TR. 2002. Osmolyte accumulation: can it really help increase crop yield under drought conditions? *Plant, Cell and Environment* **25,** 333–341.

Sharp RE, Poroyko V, Hejlek LG, Spollen WG, Springer GK, Bohnert HJ, Nguyen HT. 2004. Root growth maintenance during water deficits: physiology to functional genomics. *Journal of Experimental Botany* **55,** 2343–2351.

Sharp RE, Silk WK, Hsiao TC. 1988. Growth of the maize primary root at low water potentials: I. Spatial distribution of expansive growth. *Plant Physiology* **87,** 50–57.

Spollen WG, Sharp RE. 1991. Spatial distribution of turgor and root growth at low water potentials. *Plant Physiology* **96,** 438–443.

Spollen WG, Tao W, Valliyodan B, *et al.* 2008. Spatial distribution of transcript changes in the maize primary root elongation zone at low water potential. *BMC Plant Biology* **8,** 32.

Sponchiado BN, White JW, Castillo JA and Jones PG. 1989. Root growth of four common bean cultivars in relation to drought tolerance in environments with contrasting soil types. *Experimental Agriculture* **25,** 249–257.

Tabor CW, Tabor H. 1984. Methionine adenosyltransferase (*S*-adenosylmethionine synthetase) and *S*-adenosylmethionine decarboxylase. *Advances in Enzymology and Related Areas of Molecular Biology* **56,** 251–282.

Tabuchi A, Kikui S, Matsumoto H. 2004. Differential effects of aluminium on osmotic potential and sugar accumulation in the root cells of Al-resistant and Al-sensitive wheat. *Physiologia Plantarum* **120,** 106–112.

Tada Y, Kashimura T. 2009. Proteomic analysis of salt-responsive proteins in the mangrove plant, *Bruguiera gymnorhiza*. *Plant and Cell Physiology* **50,** 439–446.

Tezuka K, Hayashi M, Ishihara H, Onozaki K, Nishimura M, Takahashi N. 1993. Occurrence of heterogeneity of N-linked oligosaccharides attached to sycamore (*Acer pseudoplatanus* L.) laccase after excretion. *Biochemistry and Molecular Biology International* **29,** 395–402.

Thung M, Rao IM. 1999. Integrated management of abiotic stresses. In: Singh SP, ed. *Common bean improvement in the twenty-first century*. Dordrecht: Kluwer Academic Publishers, 331–370.

Toorchi M, Yukawa K, Nouri MZ, Komatsu S. 2009. Proteomics approach for identifying osmotic-stress-related proteins in soybean roots. *Peptides* **30,** 2108–2117.

Vicré M, Farrant JM, Driouich A. 2004. Insights into the cellular mechanisms of desiccation tolerance among angiosperm resurrection plant species. *Plant, Cell and Environment* **27,** 1329–1340.

Watson BS, Lei Z, Dixon RA, Sumner LW. 2004. Proteomics of *Medicago sativa* cell walls. *Phytochemistry* **65,** 1709–1720.

Werhahn W, Braun HP. 2002. Biochemical dissection of the mitochondrial proteome from Arabidopsis thaliana by three-dimensional gel electrophoresis. *Electrophoresis* **23,** 640–646.

Westgate ME, Boyer JS. 1985. Osmotic adjustment and the inhibition of leaf, root, stem and silk growth at low water potentials in maize. *Planta* **164,** 540–549.

Wisniewski M, Webb R, Balsamo R, Close TJ, Yu XM, Griffith M. 1999. Purification, immunolocalization, cryoprotective, and antifreeze activity of PCA60: a dehydrin from peach (*Prunus persica*). *Physiologia Plantarum* **105,** 600–608.

Wong YH, Lee TY, Liang HK, Huang CM, Yang YH, Chu CH, Huang HD, Ko MT, Hwang JK. 2007. KinasePhos 2.0: a web server for identifying protein kinase-specific phosphorylation sites based on sequences and coupling patterns. *Nucleic Acids Research* **35,** 588–594.

Wu Y, Cosgrove DJ. 2000. Adaptation of roots to low water potentials by changes in cell wall extensibility and cell wall proteins. *Journal of Experimental Botany* **51,** 1543–1553.

Yamaguchi M, Sharp RE. 2010. Complexity and coordination of root growth at low water potentials: recent advances from transcriptomic and proteomic analyses. *Plant, Cell and Environment* **33,** 590–603.

Yamaguchi M, Valliyodan B, Zhang J, Lenoble ME, Yu O, Rogers EE, Nguyen HT, Sharp RE. 2010. Regulation of growth response to water stress in the soybean primary root. I. Proteomic analysis reveals region-specific regulation of phenylpropanoid metabolism and control of free iron in the elongation zone. *Plant, Cell and Environment* **33,** 223–243.

Yan S, Tang Z, Su W, Sun W. 2005. Proteomic analysis of salt stress-responsive proteins in rice root. *Proteomics* **5,** 235–244.

Yang SF, Hoffman NE. 1984. Ethylene biosynthesis and its regulation in higher plants. *Annual Review of Plant Physiology* **35,** 155–189.

Yang ZB, Eticha D, Rao IM, Horst WJ. 2010. Alteration of cell-wall porosity is involved in osmotic stress-induced enhancement of aluminium resistance in common bean (*Phaseolus vulgaris* L.). *Journal of Experimental Botany* **61,** 3245–3258

Yang ZB, Eticha D, Rotter B, Rao IM, Horst WJ. 2011. Physiological and molecular analysis of polyethylene glycol-induced reduction of aluminium accumulation in the root tips of common bean (*Phaseolus vulgaris* L.). *New Phytologist* **192,** 99–113.

Yang ZB, Rao IM, Horst WJ. 2013. Interaction of aluminium and drought stress on root growth and crop yield on acid soils. *Plant and Soil* doi 10.1007/s11104-012-1580-1 (Epub ahead of print].

Zhu J, Alvarez S, Marsh EL, Lenoble ME, Cho IJ, Sivaguru M, Chen S, Nguyen HT, Wu Y, Schachtman DP, Sharp RE. 2007. Cell wall proteome in the maize primary root elongation zone. II. Region-specific changes in water soluble and lightly ionically bound proteins under water deficit. *Plant Physiology* **145,** 1533–1548.

Zhu J, Chen S, Alvarez S, Asirvatham VS, Schachtman DP, Wu Y, Sharp RE. 2006. Cell wall proteome in the maize primary root elongation zone. I. Extraction and identification of water-soluble and lightly ionically bound proteins. *Plant Physiology* **140,** 311–325.

Zörb C, Schmitt S, Mühling KH. 2010. Proteomic changes in maize roots after short-term adjustment to saline growth conditions. *Proteomics* **10,** 4441–4449.